OPEN ACCESS

African Journal of **Biotechnology**

13 June 2018
ISSN 1684-5315
DOI: 10.5897/AJB
www.academicjournals.org

ACADEMIC JOURNALS
expand your knowledge

ABOUT AJB

The African Journal of Biotechnology (AJB) (ISSN 1684-5315) is published weekly (one volume per year) by Academic Journals.

African Journal of Biotechnology (AJB), a new broad-based journal, is an open access journal that was founded on two key tenets: To publish the most exciting research in all areas of applied biochemistry, industrial microbiology, molecular biology, genomics and proteomics, food and agricultural technologies, and metabolic engineering. Secondly, to provide the most rapid turn-around time possible for reviewing and publishing, and to disseminate the articles freely for teaching and reference purposes. All articles published in AJB are peer-reviewed.

Contact Us

Editorial Office: ajb@academicjournals.org

Help Desk: helpdesk@academicjournals.org

Website: http://www.academicjournals.org/journal/AJB

Submit manuscript online http://ms.academicjournals.me/

Editorial Board

African Journal of Biotechnology

Table of Content: Volume 17 Number 24 13 June, 2018

ARTICLES

Vol. 17(24), pp. 739-747, 13 June, 2018
DOI: 10.5897/AJB2015.15190
Article Number: EA61DA457406
ISSN: 1684-5315

http://www.academicjournals.org/AJB

African Journal of Biotechnology

Full Length Research Paper

Morphological variability and molecular characterisation of thirty soybean genotypes using random amplified polymorphic DNA (RAPD) markers

Titilayo Akande[1]*, Lucky O. Omoigui[2] and Joseph Ikwebe[3]

[1]Department of Biological Sciences (Biochemistry Unit), College of Science, Federal University of Agriculture, P.M.B.2373, Makurdi, Benue State, Nigeria.
[2]Department of Plant Breeding and Seed Science, College of Agronomy, Federal University of Agriculture, P.M.B.2373, Makurdi, Benue State, Nigeria.
[3]Department of Biochemistry, Federal University, Wukari, P.M.B. 1020, Taraba State, Nigeria.

Received 22 December 2015; Accepted 30 June, 2016;

The genetic and morphological diversity of soybean germplasms was studied using random amplified polymorphic DNA (RAPD) markers and morphological traits such as plant height, height of cotyledon leaves, basal leaf length, basal leaf width, basal leaf area, terminal leaflets number, terminal leaflet length, terminal leaflet width, terminal leaflet area and basal leaf petiole length. A total of 30 germplasms were investigated. The number of amplification products obtained ranged between 6 and 9. An average of five bands was obtained per primer set. The RAPD analysis of the 30 soybean germplasms revealed a total of 23 bands, amplified by 14 different oligonucleotide primers. Sixteen of these bands were highly polymorphic with percentage polymorphism at 70%, indicating the germplasms investigated had a high level of genetic diversity. The consensus tree generated from the genetic diversity analysis placed the soybean germplasms into five groups at an agglomerate coefficient of 0.6 (similarity level). Similarly, cluster analysis from the morphological characterisation revealed 5 clades with an average distance between clusters of 0.75. There was a significant lack of correlation between the RAPD markers and the morphological traits evaluated. Although, both analyses grouped the soybean genotypes into 5 clades, the composition of the individual clusters were very variable and divergent with the correlation between the largest clusters in the molecular and morphological characterisation at only 35-42%.

Key words: Soybean, germplasm, random amplified polymorphic DNA (RAPD), genetic diversity, morphological variability, polymorphism.

INTRODUCTION

Soybean (*Glycine max*) is a leguminous plant. It originated from Asia and presently, China and United States of America are the world's largest producers (FAO, 2011). In Nigeria, soybean cultivation started since 1928 and presently, Benue, Niger and some parts of Kaduna States are the major producing areas in the

country. As a single seasonal crop, it is grown in middle of June and harvested at the beginning of dry season (October – November) to avoid field losses (International Institute for Tropical Agriculture- IITA, 2009).

The advent of molecular biology has revolutionized the field of plant systematics and has been used successfully in establishing phylogenetic relationships at all taxonomic levels (Bohs, 2005). It has also been used in DNA fingerprinting of plant genomes (Cervera et al., 1998) and in genetic diversity studies (Isshiki et al., 2008). The use of molecular techniques in genetic diversity studies is supported by the finding that evolutionary forces such as natural selection and genetic drift produce divergent phylogenetic branching which can be recognized because the molecular sequences on which they are based, share a common ancestor (Singh et al., 2010). A number of genetic maps have been developed for soybean with several types of molecular markers. Hwang et al. (2009) mapped 1810 simple sequence repeats (SSR) site markers in some recombinant inbred populations of soybean, from which they constructed high-density linkage maps.

Random amplified polymorphic DNA (RAPD), when compared with other molecular markers, is more effective in this regard as it is simple, rapid, requires only a small quantity of DNA and it is well adapted for nonradioactive DNA fingerprinting of genotypes (Cao et al., 1999). It is also able to generate numerous polymorphisms (Williams et al., 1990). More recent studies have used molecular markers to identify genetically diverse plant introductions to be used for crosses in cultivar improvement programs (Thompson and Nelson, 1998a, b; Thompson et al., 1998; Narvel et al., 2000). These studies have had more success than conventional selection programs in producing productive lines from plant introductions crossed with elite genotypes. Khare et al. (2013) used RAPD to investigate the genetic diversity and relatedness of 38 soybean germplasms; they found 259 RAPD marker loci with 253 of them polymorphic. Perić et al. (2014) compared three methods in the assessment of diversity in soybean, and RAPD was found to be more superior in assessing differences among genetically similar genotypes. Alamri (2014) also studied inter simple sequence repeat (ISSR) and RAPD markers in detecting genetic variation in soybean. The results revealed that the levels of polymorphic loci detected with the two marker systems were in general moderate and similar. Very recently, Pakyürek and Akçin (2015) also used RAPD markers to study genetic diversity in seven different soybean cultivars, the results revealing significant polymorphisms. In Nigeria, not much has been done on the nature of genetic diversity and characterization of *Glycine max*, especially using molecular tools. There is a need for extensive evaluation of new germplasms found in Nigeria to determine their genetic diversity.

This research work aimed to assess the morphological variability and molecular diversity of soybean (*Glycine max*.) using RAPD markers.

MATERIALS AND METHODS

Thirty soybean germplasms (representing several independent breeding sources from IITA) used in this study were obtained from Molecular Biology Laboratory, University of Agriculture, Makurdi, Benue State, Nigeria. The soybean germplasms are shown in the Table 1.

Planting of soybean germplasms

Three seeds of each germplasm were planted in plastic pots and thinned to two stands per pot at seven days after planting.

Collection of DNA sample on Fast Technology Application (FTA) Plant card (Whatman, 2014)

Young leaves of soybean at 14 days after planting were excised from the plants. Depending on the size of the leaves, either whole leaves or portions of the leaves were mechanically crushed and disrupted on FTA plantsaver cards using porcelain pestle. The crushed leaves on FTA plantsaver cards were air-dried at room temperature for 1 h. Afterwards, 2 mm circles of FTA plantsaver cards containing leaf tissue were collected using a Harris Micro-Punch (Life Technologies) and was transferred into a thin-wall micro centrifuge tubes.

Preparation of plant genomic DNA

200 µl of FTA purification reagent was added to each of the micro centrifuge tubes from above. The micro centrifuge tubes were vortex and mixed for 1–2 s at low speed. The tubes were incubated at room temperature for 5 min, and the wash solution was discarded. The washes were repeated with FTA reagents 2 more times, followed by 2 more washes with 1TE buffer (10 mmol/L Tris, 0.1 mmol/L ethylene diamine tetracetic acid (EDTA), pH 8.0). The FTA paper cards were air-dried at room temperature for 1 h, and the paper punches placed directly into PCR reagents for analysis using the method of Lin et al. (2000) and Omoigui et al. (2011).

Polymerase chain reaction (PCR) protocol

Aliquots of DNA samples from each genotype were amplified with

*Corresponding author. E-mail: titilayomi2013@gmail.com. Tel: +23408020790765.

Table 1. List of soybean germplasms.

S/N	Genotype
1	TGX 1989-11F
2	TGX 1990-110FN
3	TGX 1989-42F
4	TGX 1990-95F
5	TGX 1989-45F
6	TGX 1989-53FN
7	TGX 1993-4FN
8	TGX 1989-75FN
9	TGX 1990-78F
10	TGX 1990-114FN
11	TGX 1987-62F
12	TGX 1448-2E
13	TGX 1989-40F
14	TGX 1990-52F
15	TGX 1989-48FN
16	TGX 1990-40F
17	TGX 1989-49FN
18	TGX 1990-57F
19	TGX 1989-68FN
20	TGX 1990-46F
21	TGX 1990-55F
22	TGX 1987-10F
23	TGX 1935-10F
24	TGX 1485-1D
25	TGX 1945-1F
26	TGX 1951-3F
27	TGX 1935-3F
28	TGX 1904-6F
29	TGX 1951-4F
30	TGX 1955-4F

each of the 14 oligonucleotide primers (Inqaba Inc. South Africa) listed in Table 2 using a thermal cycler. The PCR were carried out in 25 µl volumes containing 6.5 µl of 10 × Taq buffer, 4 µl of 2 mM dNTP mix, 1 µl primer, 1 µl of Taq polymerase, 1 µl $MgCl_2$, 10.5 µl Nuclease-free water and 1 µl template DNA. The PCR method has an initial denaturation step at 94°C for 5 min, followed by 44 cycles of 94°C for 1 min, 35°C for 1 min, and 72°C for 2 min. A final extension step was given at 72°C for 7 min (Mundewadikar and Deshmukh, 2014). The reaction was repeated two times for each selected primer.

Gel electrophoresis

The PCR products were electrophoresed on 2% agarose gel in a horizontal gel electrophoresis tank. 10 µl of DNA ladder and 16 µl of PCR product were loaded on the gel and resolved for about 40 min. The gel was stained with ethidium bromide and visualized on a Benchtop UV transilluminator and photographed with digital camera for scoring.

Table 2. List of primers used for RAPD analysis.

S/N	Primer name	Primer sequence (5' – 3')
1	OPA-01	CAGGCCCTTC
2	OPA-02	TGCCGAGCTG
3	OPA-03	AGTCAGCCAC
4	OPA-04	AATCGGGCTG
5	OPA-05	AGGGGTCTTG
6	OPA-07	GAAACGGGTG
7	OPA-08	GTGACGTAGG
8	OPA-09	GGGTAACGCC
9	OPA-10	GTGATCGCAG
10	OPC-01	TTCGAGCCAG
11	OPC-02	GTGAGGCGTC
12	OPC-05	GATGACCGCC
13	OPC-07	GTCCCGACGA
14	OPC-08	TGGACCGGTG

Scoring and data analysis

The data for RAPD analysis were scored from digital photographs of ethidium bromide-stained agarose gels using the Ultraviolet Bench Top illuminator. DNA bands were considered to be similar if they occurred exactly at the corresponding position on the gel. Band size was determined by comparing with a standard DNA ladder run alongside the soybean genotypes. An RAPD band profile, presence (1) or absence (0) was recorded into a binary matrix. This matrix was subjected to genetic similarity analysis using root mean square distance (RMSD) coefficient, and clustering was done using a dendrogram constructed by an Unweighted Paired group Method using Arithmetic Averages (UPGMA) (Garcia et al., 1999).

Morphological characterisation

The morphological traits analyses were carried out at three weeks of planting. Parameters measured in centimetres included: Plant height, height of cotyledon leaves, basal leaf length, basal leaf width, basal leaf area, terminal leaflets number, terminal leaflet length, terminal leaflet width, terminal leaflet area and basal leaf petiole length. Plant height was measured from ground level to stem tip for three plants and mean plant height was recorded. Cotyledon height was measured from ground level to cotyledon tip, for three plants and mean cotyledon height was recorded. Basal leaf length was measured from lamina tip to the point of intersection of the lamina and stem and basal leaf width was measured from tip to tip between the widest lamina. The leaf area (basal and terminal) of each leaf was calculated using the method described by Pandy and Singh (2011). Data generated was subjected to hierarchical clustering using UPGMA, and a dendrogram was generated for the 10 traits studied using SAS 9.3.

RESULTS

The RAPD analysis of the 30 samples revealed a total of23 bands (Table 3). Sixteen of these bands were highly

Table 3. Analysis of RAPD banding pattern for soybean germplasms.

Primer set	Total number of bands	Number of polymorphic bands	Percentage polymorphic bands (%)
OPA-01, OPA-02, OPA-03 and OPA-04	6	5	83.3
OPA-05, OPA-07, OPA-08 and OPA-09 and OPA-10	9	3	33.3
OPC-01, OPC-02, OPC-05, OPC-07 and OPC-08	8	8	100
Total	23	16	70
Average	7.7	5.3	

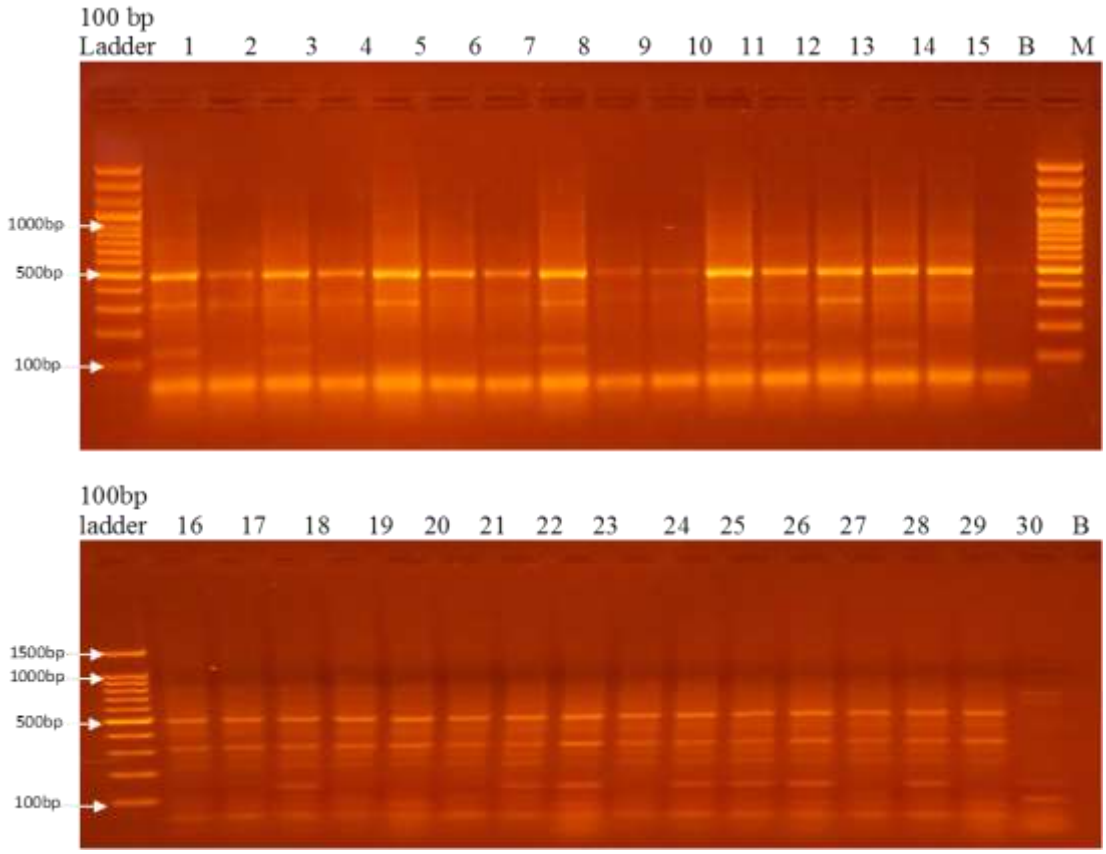

Figure 1. Band profile of multiplex OPA-01, OPA-02, OPA-03 and OPA-04 Primers. 100 bp DNA ladder serves as reference point; B represents the blank; 1 to 30 corresponds to bands produced by the amplified DNA from 30 soybean germplasms studied.: 1=TGX 1935-3F; 2=TGX 1987-62F; 3=TGX 1990-78F; 4=TGX 1993-4FN; 5= TGX 1989-45F; 6=TGX 1904-6F; 7= TGX 1990-40F; 8= TGX 1989-68FN; 9= TGX 1990-52F; 10=TGX 1990-57F; 11= TGX 1989-42F; 12= TGX 1990-55F;13= TGX 1835-10E; 14= TGX 1990-95F; 15= TGX 1990-114FN; 16= TGX 1989-53FN;17= TGX 1448-2E; 18= TGX 1990-46F; 19= TGX 1987-10F; 20= TGX 1485-1D; 21= TGX 1945-1F; 22= TGX 1951-4F;23=TGX 1990-110FN, 24=1989-11F; 25=1989-40F; 26=TGX 1955-4F; 27= TGX 1989-48FN; 28= TGX 1951-3F; 29= TGX 1989-49FN and 30= TGX 1989-75FN. The band fragments of multiplex of OPA-05, OPA-07, OPA-08, OPA-09 and OPA-10 primers ranged from 100 to 110 bp or 1.1 kbp

polymorphic with percentage polymorphism at 70%. The amplified band sizes varied between 100 and 1100 bp. The numbers of amplification products obtained were in the range 6 to 9. Multiplex of OPA-01, OPA-02, OPA-03 and OPA-04 primers produced the minimum number of polymorphic bands (6), OPA-05, OPA-07, OPA-08 and OPA-09 primers produced the highest number of polymorphic bands (9) and multiplex of OPA-10, OPC-01, OPC-02, OPC-05 and OPC-07 primers produced 8 polymorphic bands representing 100% polymorphism. An average of 5 bands was also obtained per primer set. Figures 1 to 3 show the band profiles of RAPD markers

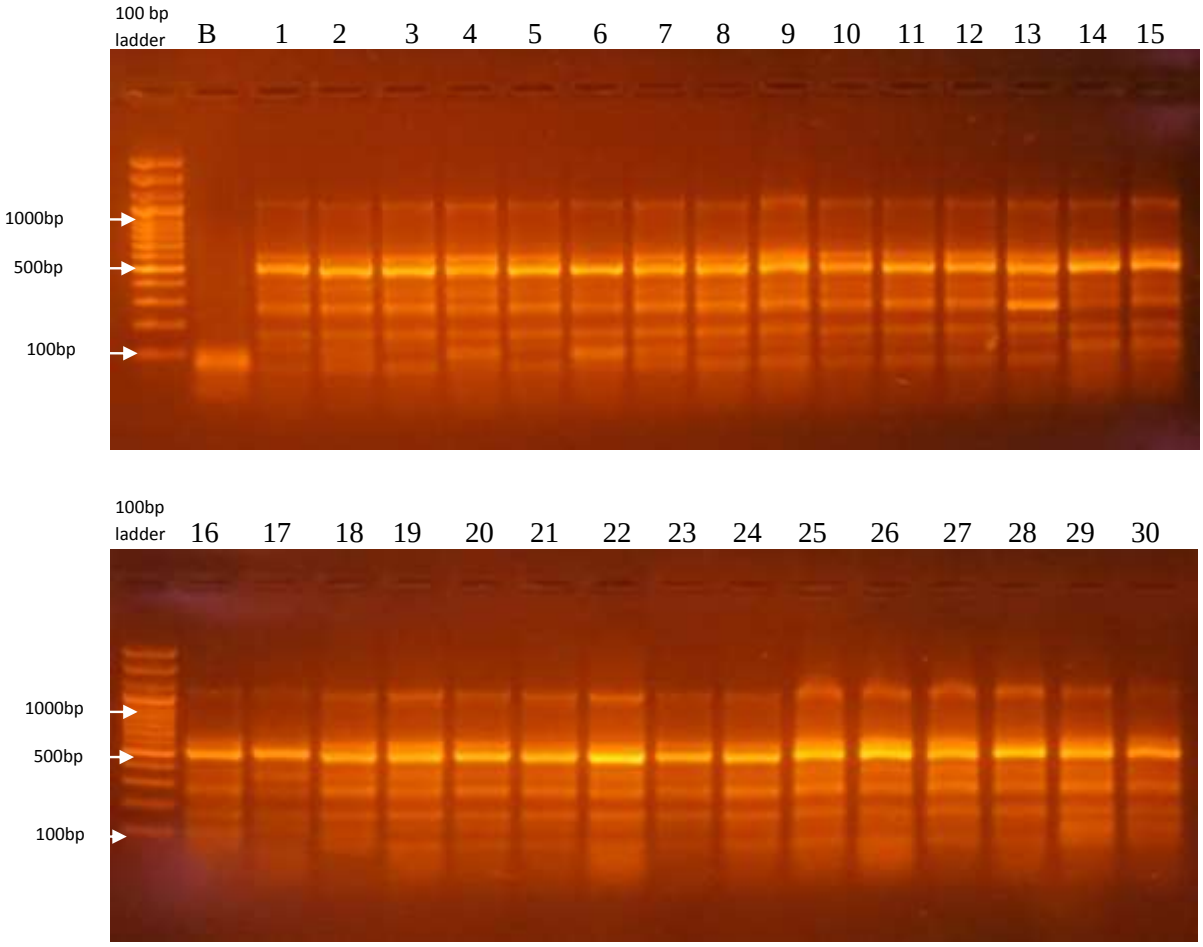

Figure 2. Band profile of multiplex OPA-05, OPA-07, OPA-08, OPA-09 primers and OPA-10. 1=TGX 1935-3F; 2=TGX 1987-62F; 3=TGX 1990-78F; 4=TGX 1993-4FN; 5= TGX 1989-45F; 6=TGX 1904-6F; 7= TGX 1990-40F; 8= TGX 1989-68FN; 9= TGX 1990-52F; 10=TGX 1990-57F; 11= TGX 1989-42F; 12= TGX 1990-55F; 13= TGX 1835-10E; 14= TGX 1990-95F; 15= TGX 1990-114FN; 16= TGX 1989-53FN;17= TGX 1448-2E; 18= TGX 1990-46F; 19= TGX 1987-10F; 20= TGX 1485-1D; 21= TGX 1945-1F; 22= TGX 1951-4F; 23= TGX 1990-110FN, 24=1989-11F; 25=1989-40F; 26=TGX 1955-4F; 27= TGX 1989-48FN; 28= TGX 1951-3F; 29= TGX 1989-49FNand 30= TGX 1989-75FN. The band fragments of Multiplex OPC-01, OPC-02, OPC-05, OPC-07 and OPC-08 primers ranged from 150 bp to 700 bp.

for the thirty soybean germplasms studied. The band fragments of multiplex OPA-01, OPA-02, OPA-03 and OPA-04 primers ranged from 120 to 500 bp.

Figure 4 represents the distance matrix tree from the RAPD markers showing the degree of genetic diversity and/or relatedness of the 30 soybean germplasms. The consensus tree generated placed the soybean germplasms into 5 groups at an agglomerate coefficient of 0.6 (similarity level). Cluster 1 revealed the genetic relatedness of 5 germplasms namely, TGX 1935-3F, TGX 1989-45F, TGX 1990-95F, TGX 1990-114FN and TGX 1989-75FN. Cluster 2 comprised of six germplasms namely, TGX 1987-62F, TGX 1989-53FN, TGX 1990-46F, TGX 1989-49FN, TGX 1993-4FN and TGX 1904-6F. Cluster 3 being the cluster with the largest germplasms comprised of 18 closely related germplasms namely, TGX 1990-78F, TGX 1989-42F, TGX 1989-68FN, TGX 1990-55F, TGX 1448-2E, TGX 1945-1F, TGX 1951-4F, TGX 1935-10E, TGX 1987-10F, TGX 1485-1D, TGX 1989-48FN, TGX 1990-52F, TGX 1990-57F and TGX 1990-40F. Cluster 4 comprised of 3 germplasms namely, TGX 1989-40F, TGX 1955-4F and TGX 1951-3F. Lastly, cluster 5 consisted of 2 germplasms (TGX 1989-11F and TGX 1990-110FN) which are outliers that are genetically different from all other germplasms.

Similarly, cluster analysis from the morphological characterisation of the soybean germplasms (Figure 5) revealed 5 clades with an average distance between clusters of 0.75. Cluster 1 comprised ten germplasms namely, TGX 1448-2E, TGX 1989-48FN, TGX 1951-3F,

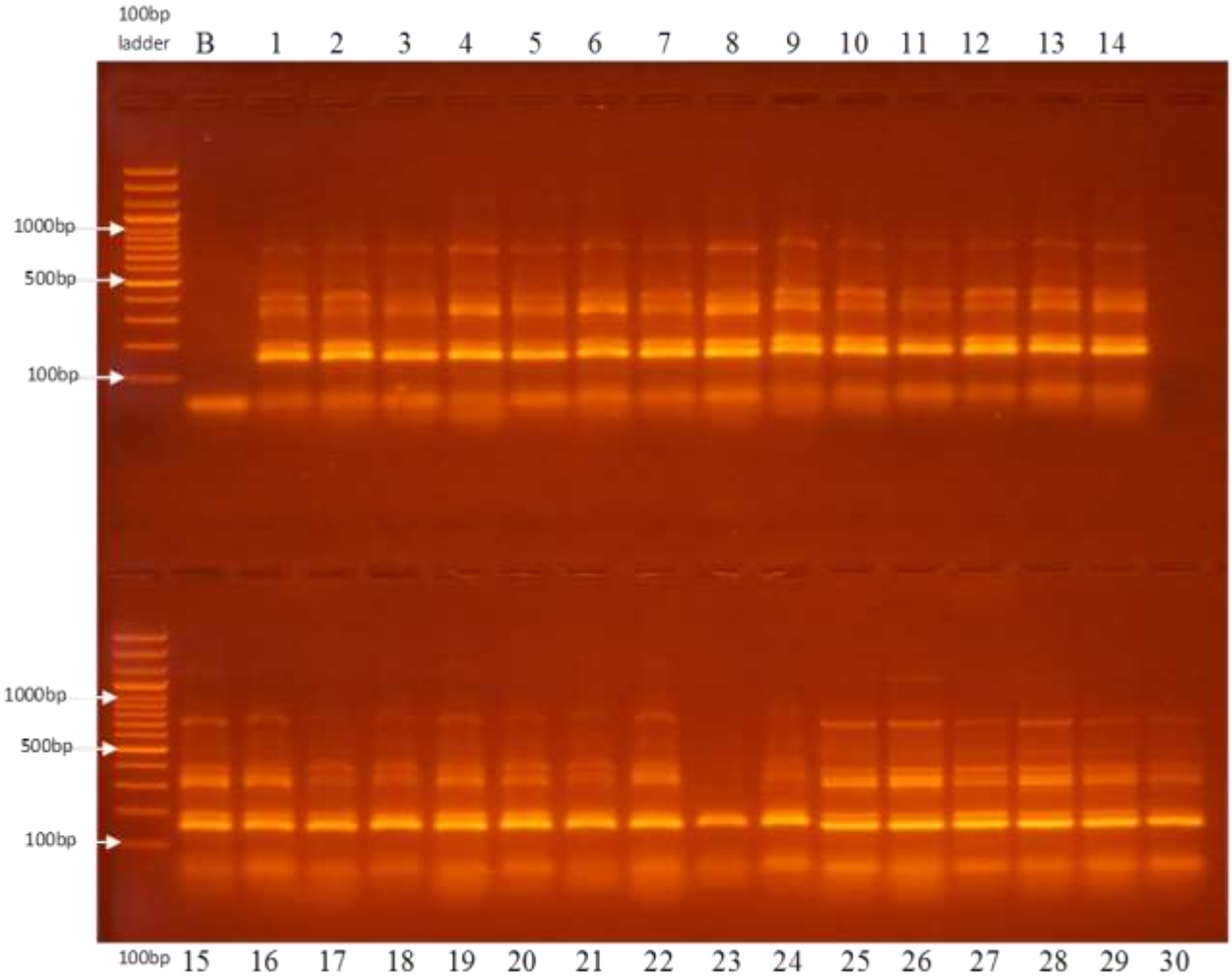

Figure 3. Band Profile of Multiplex OPC-01, OPC-02, OPC-05, OPC-07 and OPC-08 primers. 1=TGX 1935-3F; 2=TGX 1987-62F; 3=TGX 1990-78F; 4=TGX 1993-4FN; 5= TGX 1989-45F; 6=TGX 1904-6F; 7= TGX 1990-40F; 8= TGX 1989-68FN; 9= TGX 1990-52F; 10=TGX 1990-57F; 11= TGX 1989-42F; 12= TGX 1990-55F; 13= TGX 1835-10E; 14= TGX 1990-95F; 15= TGX 1990-114FN; 16= TGX 1989-53FN;17= TGX 1448-2E; 18= TGX 1990-46F; 19 TGX 1987-10F; 20= TGX 1485-1D; 21= TGX 1945-1F; 22= TGX 1951-4F; 23= TGX 1990-110FN, 24=1989-11F; 25=1989-40F; 26=TGX 1955-4F; 27= TGX 1989-48FN; 28= TGX 1951-3F; 29= TGX 1989-49FN and 30= TGX 1989-75FN.

TGX1989-68FN, TGX 1990-52F, TGX 1989-45F, TGX 1935-3F, TGX 1993-4FN, TGX 1990-46F and TGX 1989-53FN. Four germplasms namely, TGX 1485-1D, TGX 1990-46F, TGX 1989-49FN and TGX 1990-55F were grouped into cluster 2. Cluster 3 consists of twelve germplasms that are morphologically related namely, TGX 1835-10E, TGX 1990 -40F, TGX 1989-11F, TGX 1990-110FN, TGX 1990-57F, TGX 1945-1F,TGX 1989-40F, TGX 1990-114FN, TGX 1951-4F, TGX 1987-10F, TGX 1989-42F and TGX 1990-95F. Cluster 4 has three germplasms namely, TGX 1987-62F, TGX 1955-4F and TGX 1990-78F. Also, the dendrogram shows that cluster 5 consists of an outlier (TGX 1989- 75F) that is morphologically different from all other germplasms.

DISCUSSION

The high degree of polymorphism revealed by the RAPD markers was further accentuated by the observation fromthe cluster analysis. The molecular characterization of the 30 soybean germplasms with RAPD markers revealed 70% polymorphism, indicating a high level of genetic diversity in the soybean germplasms investigated. This result also shows that the RAPD markers were highly polymorphic and informative. The result is in

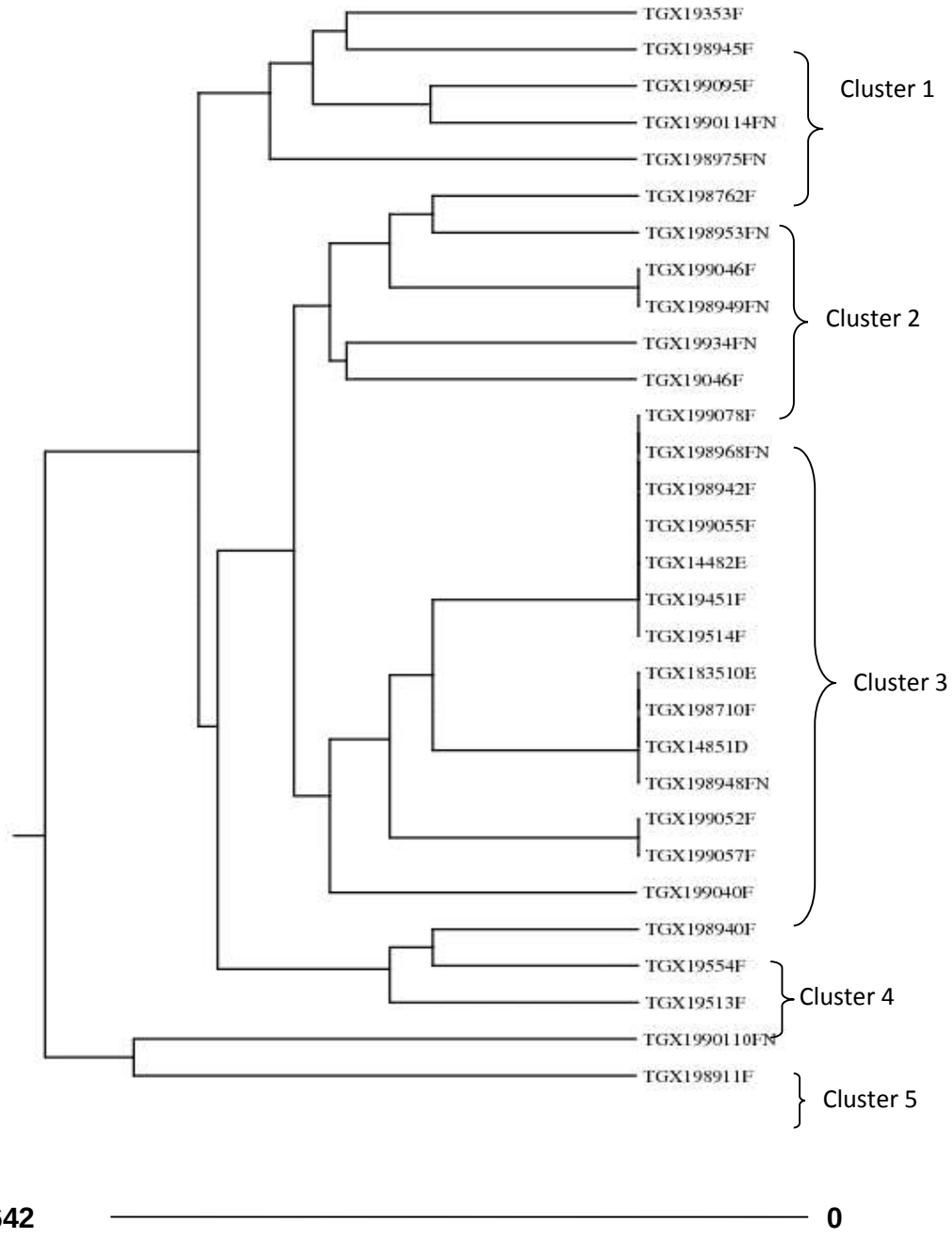

Figure 4. Dendrogram of all RAPD primers showing the genetic diversity amongst thirty soybean germplasms using UPGMA method (distance matrix using RMSD coefficient).

agreement with the report of Chowdhury et al. (2001) that RAPD markers are efficient for measuring genetic diversity and relatedness as well as identifying varieties of soybeans. This is the first report of genetic diversity analysis of advanced soybean genotypes (breeding lines) in Nigeria using RAPD markers. This result is in concordance with the previous reports of Singh et al. (2008) who reported 89.9% polymorphism, while Li and Nelson (2005) reported 56% polymorphism in their studies using RAPD primers. However, Thompson et al. (1998) observed a low level (36%) of DNA variation among 35 soybean genotypes using RAPD primers. Conflicting reports on the extent of observed polymorphism in soybean in different studies could be

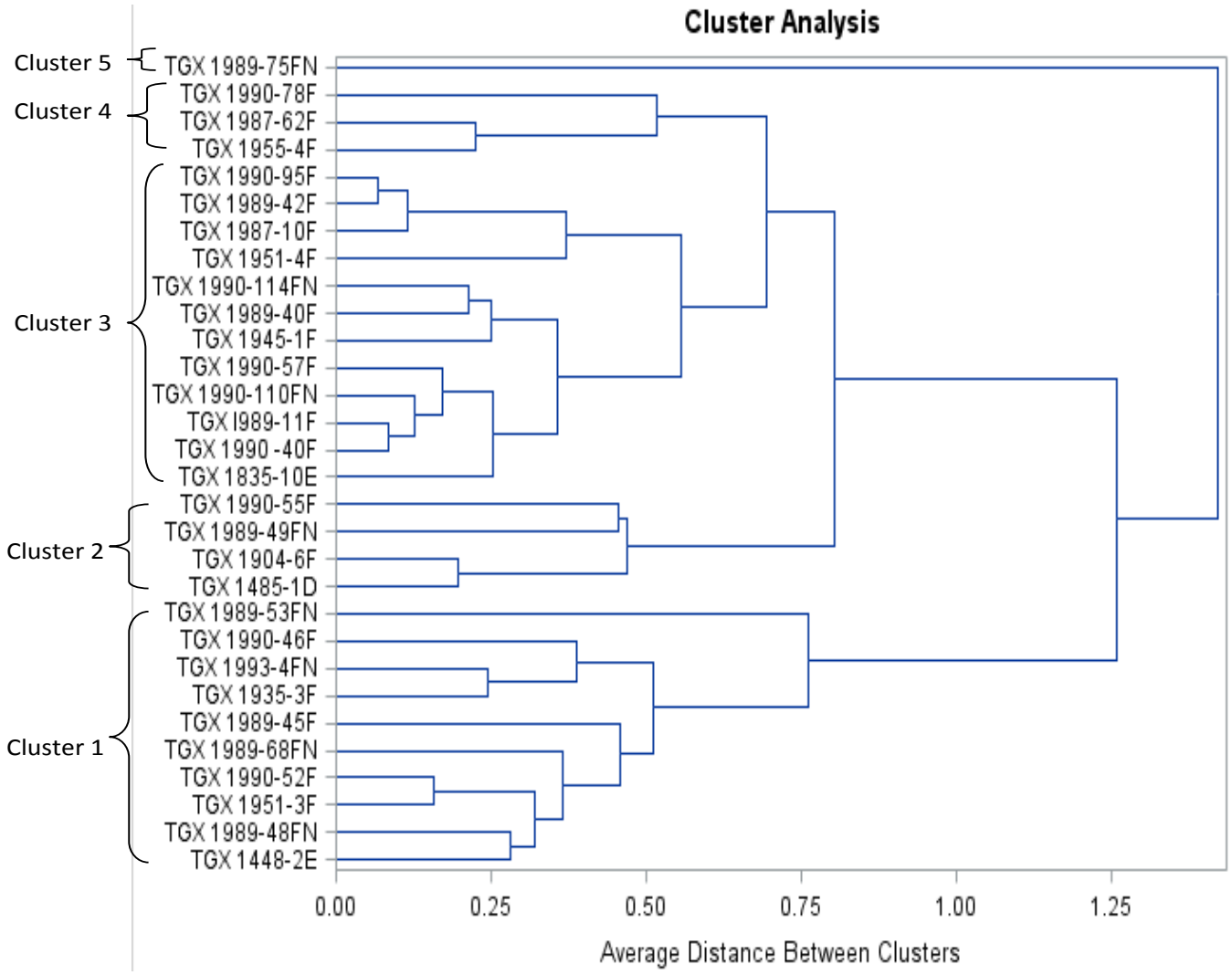

Figure 5. Dendrogram of morphological traits.

attributed to the unique nature of the genetic materials under investigation and sequences of the primers.

There was a significant lack of correlation between the RAPD markers and the morphological traits evaluated. Although, both analyses grouped the soybean genotypes into 5 clades, the composition of the individual clusters were very variable and divergent. For example, cluster 3 was the largest cluster in both cases with 12 and 14 members for genetic and morphological relatedness respectively but, the correlation was only 35-42% (TGX 1989-42F, TGX 1987-10F, TGX 1951-4F, TGX 1945-1F and TGX 1990-57F). Furthermore, whereas TGX 1990-110FN and TGX 1989-11F were outliers and genetically distinct and distant from the other germplasms in the RAPD dendrogram, they were shown to be morphologically related to at least 10 other germplasms in cluster 3. Also, TGX 1989-75FN was morphologically different to all the other germplasms and hence an outlier in the dendrogram. In the genetic characterisation however, it was shown to be genetically related to 4 other germplasms in cluster 1. This lack of correlation between genetic and morphological diversity have been previously reported in other plant species (Doebley, 1989). It could well be as Zannou et al. (2008) surmised that during the process of domestication, modifications in a few genes can lead to marked phenotypic differences.

In terms of morphological characterisation, this study agrees with several earlier studies on soybean using morphological markers (Malek et al., 2014; Ojo et al., 2012; Iqbal et al., 2008; Cui et al., 2001) such as branch number, plant height, pod number and seed weight, seed shape, seed eye colour, yield, etc. which have all provided useful information for proper classification of soybean germplasms.

Conclusion

Summarily, this study reveals the presence of significant genetic variability in the 30 soybean genotypes investigated. Genetic diversity and/or relationship assessments could provide useful information for efficient utilization of these germplasms, especially during future improvement programmes. This result also showed that the RAPD markers were highly polymorphic and informative, clearly grouping the genotypes into distinct clusters. Although, the correlation between the largest clusters in the molecular and morphological characterisation was only 35-42%, enlarging the sample size in subsequent investigations could provide a clearer picture and perhaps better information between the two. Nevertheless, advanced breeding lines of soybean which have undergone cycles of artificial selection, should not be neglected when further improvement of soybean is considered.

CONFLICT OF INTERESTS

The authors declare that there is no conflict of interests regarding the publication of the paper.

REFERENCES

Alamri S (2014). Comparative analysis of soybean (*Glycine max*) accessions using inter simple sequence repeat (ISSR) and randomly amplified polymorphic DNA (RAPD) markers. MSc. Thesis. The School of Graduate Studies, Laurentian University, Sudbury, Ontario, Canada.

Bohs L (2005). Revision of Solanium section. Syst. Bot. Monog. 61:1141-1155.

Cao W, Scoles G, Hucl P, Chibbar RN (1999). The use of RAPD analysis to classify *Tritcum* accessions. Theor. Appl. Genet. 98:602-607.

Cervera MT, Cabezas JA, Sancha JC, Martinez de Toda F, Martinez-Zapater JM (1998). Application of AFLPs to the Characterization of grapevine genetic resources. A case study with Accession from Rioja (Spain). Theor. Appl. Genet. 97:51-59.

Chowdhury AK, Srinives P, Tongpamnak P, Saksoon P (2001). Genetic diversity based on morphology and RAPD analysis in vegetable soybean. Kor. J. Crop Sci. 46(2):112-120.

Cui Z, Carter Jr. TE, Burton JW, Wells R (2001). Phenotypic diversity of modern Chinese and North American soybean cultivars. Crop. Sci. 41(6):1954-1967.

Doebley J (1989). Isozyme evidence and evolution of crop plants. In: Isozymes in Plant Biology. Soltis DE, Soltis PS (Eds.). Dioscorides Press, Portland, OR. pp. 165-191.

Food and Agriculture Organization of the United Nations (FAO) Production Yearbooks (1988 to 2011).

Food and Agriculture Organisation of the United Nations. FAO Statistics Division, FAOSTAT database (2011).

Hwang TY, Sayama T, Takahashi M, Takada Y, Nakamoto Y, Funatsuki H, Hisano H, Sasamoto S, Sato S, Tabata S, Kono I, Hoshi M, Hanawa M, Yano C, Xia Z, Harada K, Kitamura K, Ishimoto M (2009). High-density Integrated Linkage Map Based on SSR Markers in Soybean. DNA Res. 16:213-225.

International Institute of Tropical Agriculture (IITA) (2009). Genetic Resources for Tropical Agriculture, Pamphlet, P 32.

International Institute of Tropical Agriculture–IITA (2009): Soybean crop.

Isshiki S, Iwataa N, Khana MMR (2008). ISSR variations in *Solanium melongena* L. and related species. Sci. Hort. 117:186-190.

Iqbal Z, Arshad M, Ashraf M, Mahmood T, Waheed A (2008). Evaluation of soybean [*Glycine max* (L.) Merrill] germplasms for some important morphological traits using multivariate analysis. Pak. J. Bot. 40(6):2323-2328.

Khare D, Bisen A, Nair P, Tripathi N (2013). Genetic diversity in soybean germplasms identified by RAPD markers. AsPac J. Mol. Biol. Biotechnol. 21(3):121-123.

Lin JJ, Fleming R, Kuo J, Mathews BF, Saunders JA (2000). Detection of plant genes using a rapid, nonorganic DNA purification method. Biotech. 28: 346-350.

Malek MA, Rafii MY, Afroz MSS, Nath UK, Mondal MMA (2014). Morphological characterization and assessment of genetic variability, character association, and divergence in soybean mutants. Sci. W. J. 12 p.

Mundewadikar DM, Deshmukh PR (2014). Genetic variability and diversity studies in soybean [*Glycine max* (L.) Merrill] using RAPD Marker. Int. J. Sci. Res. Pub. 4(9):1-4.

Ojo DK, Ajayi AO, Oduwaye OA (2012). Genetic relationships among soybean accessions based on morphological and RAPDs techniques. Pert. J. Trop. Agric. Sci. 35(2):237-248.

Omoigui LO, Ishiyaku MF, Ousmane B, Gowda BS, Timko MP (2011). Application of Fast Technology for analysis (FTA) for sampling and recovery of Deoxyribonucleic acid (DNA) for molecular characterization of cowpea breeding lines for *Striga* resistance. Afr. J. Biotechnol. 10(85):19681-19986.

Pakyürek M, Akçin A (2015). Determination of Genetic Polymorphism among Soybean (*Glycine max*. L. Merrill) Cultivars Developed in Recent Years through RAPD Markers. Int. J. Sec. Metabol. 2(1):3-7.

Perić V, Nikolić A, Babić V, Sudarić A, Srebrić M, Dordević V, Drinić SM (2014). Genetic relatedness of soybean genotypes based on agromorphological traits and RAPD markers. Genetika 46(3):839-854.

Singh RJ, Nelson RL, Chung G (2006). Genetic Resources, Chromosome Engineering, and Crop Improvement: Oilseed Crops, Vol. 4. London: Taylor & Francis. P 15.

Singh RK, Bhatia VS, Yadav S, Athale R, Lakshmi N, Guruprasad KN, Chauhan GS (2008). Identification of genetically diverse genotypes for photoperiod insensitivity in soybean using RAPD Markers. Physiol. Mol. Biol. Plants. 14(4):369-375.

Singh RK, Mishra SK, Singh SP, Mishra N, Sharma ML (2010). Evaluation of microsatellite markers for genetic diversity analysis among sugarcane species and commercial hybrids. Aust. J. Crop Sci. 4:116-125.

Thompson JA, Nelson RL (1998). Utilization of diverse germplasms for soybean yield improvement. Crop Sci. 38:1362-1368.

Thompson TA, Nelson RL, Vodkin LO (1998). Identification of diverse Soybean germplasm using RAPD markers. Crop Sci. 38(5):1348-1355.

Whatman (2014). Protocol on Plant DNA extraction using FTA Plantsaver method.

Williams JGK, Kubelik AR, Refalski JA Tingey SV (1990). DNA Polymorphisms amplified by arbitrary primers are useful as genetic markers. Nucl. Acids Res. 18:6531-6535.

Zannou A, Kossou D K, Ahanchede A, Zoundjihekpon J, Agbicodo E, Struik PC, Sanni A (2008). Genetic variability of cultivated cowpea in Benin assessed by random amplified polymorphic DNA. Afr. J. Biotechnol. 7(24):4407-4417.

Vol. 17(24), pp. 748-752, 13 June, 2018
DOI: 10.5897/AJB2017.16119
Article Number: 637892A57418
ISSN: 1684-5315

http://www.academicjournals.org/AJB

African Journal of Biotechnology

Full Length Research Paper

Surface plasmon resonance and antimicrobial properties of novel silver nanoparticles prepared from some indigenous plants in Uyo, Nigeria

Tenderwealth Clement Jackson[1*], Bernard Opatimidi Patani[2] and Ntiido Ndifreke Udosen[1]

[1]Department of Pharmaceutics and Pharmaceutical Technology, University of Uyo, Akwa Ibom State, Nigeria.
[2]Nigerian Agip Oil Company, Port Harcourt, Rivers State, Nigeria.

Received 20 June, 2017; Accepted 29 September, 2017

Synthesis of nanoparticles was done by green method. Aqueous extracts of *Vernonia amygdalina, Telferia occidentalis* and *Lasianthera africana* were used as the model vegetables. Silver nitrate was used as the silver precursor, while the plant extracts served as the reducing agents and Xanthan gum (0.25, 0.5, 0.75 and 1.00% w/v) was introduced as stabilizing agents. Twelve batches of silver nanoparticles were synthesized: 0.25% *V. amygdalina*, 0.50% *V. amygdalina*, 0.75% *V. amygdalina*, 1.00% *V. amygdalina*, 0.25% *T. occidentalis*, 0.5% *T. occidentalis*, 0.75% *T. occidentalis*, 1.00% *T. occidentalis*, 0.25% *L. africana*, 0.50% *L. africana*, 0.75% *L. africana*, and 1.00% *L. africana*. The nanoparticle formation was confirmed with the visible colour change from colourless to characteristic reddish brown and the plasmon resonance peak ranges from 350 to 500 nm. The surface plasmon resonance (SPR) characteristic peak for synthesized nanoparticles gave values from 371 to 452 nm. Nanoparticles synthesized from *V. amygdalina* and *T. occidentalis* had similar ($p > 0.05$) peaks for the surface plasmon resonance. Nanoparticles synthesized from *L. africana* had the least SPR (371 nm). After 9 months of storage, SPR and colour of nanoparticles remain unchanged. The antimicrobial activities of these nanoparticles were studied against *Escherichia coli, Staphylococcus aureus, Pseudomonas aeruginosa,* and *Bacillus subtilis.* They had satisfactory inhibitions against the four test microorganisms. Among the different vegetables used in the study, *L. africana* had the highest sensitivity.

Key words: Silver nanoparticles, green method, characterisation, antimicrobial.

INTRODUCTION

The use of plants for the preparation of nanoparticles has gained more relevance in the last decade as the technique is simple and involves the use of plants extracts which contain biomolecules of medicinal value (Roy and Das, 2015). Extensive researches have been carried out on silver nanoparticles as a major group of nanomaterials.

*Corresponding author. E-mail: clementjackson1@gmail.com.

They have attracted a great deal of attention due to their peculiar physico-chemical, optical and biological properties (Rao and Tang, 2017). Nano silver has immense applications in the field of detection, diagnostics, therapeutics, and antimicrobial activity (Sachin et al., 2012).

Various chemical and physical methods have been developed to prepare silver nanoparticles (AgNPs). Among them, the chemical reduction is the most widely used. These approaches are usually associated with the use of hazardous chemicals such as reducing agent, stabilizers, and organic solvents. This may also involve special requirements for the employed techniques such as high energy radiation and microwave irradiation (Rao and Tang, 2017). Some physical and chemical techniques used in the preparation of AgNPs have also been reported (Yang et al., 2011; Korbekandi and Abbasi, 2009). Many of these methods are either expensive or involve the use of harmful chemicals. Therefore, there is an increasing need to develop the eco-friendly, nontoxic and cost-effective methods for the preparation of AgNPs without the application of toxic chemicals and special equipments. In recent years, the biological approaches using microorganisms and plant extracts have become valuable alternatives to chemical synthesis.

The synthesis of silver nanoparticles has been carried out using fruit rind extract of *Citrullus lanatus* (Ndikau et al., 2017). Synthesis of silver nanoparticles have also been done using *Murraya koenigii* (Jackson et al., 2016), *Pulicaria glutinosa* (Khan et al., 2013), *Eriobotrya japonica* leaf extract (Rao and Tang, 2017), and apple extract (Ali et al., 2016). The preparation of silver nanoparticles using *Cinnamomum camphora* (Xin et al., 2010) and *Nicotiana tobaccum* (Kumar et al., 2011) has been found in literature. Seaweed (Ganesan et al., 2013a) and enzymes (Ganesan et al., 2013b) have also been employed in silver nanoparticle preparation.

In spite of all these researches, there is dearth of information on the synthesis of silver nanoparticles using xanthan in addition to edible plants, hence, the need for this study with the following objectives; to prepare aqueous extract of some edible plants (*Vernonia amygdalina, Telfaria occidentalis,* and *Lasianthera africana*) and use the extracts as reducing agents in the synthesis of silver nanoparticles. The antimicrobial properties of the nanoparticles were also determined.

MATERIALS AND METHODS

Xanthan gum (Sigma Aldrich, USA), silver nitrate (BDH Chemicals, England), and plant extract (*T. occidentalis, V. amygdalina,* and *L. africana*) were the materials used. Other chemicals and reagents were of laboratory grade.

Preparation of plant extract

Fresh leaves of *V. amygdalina* (bitter leaf), *L. africana* (editan leaf) and *T. occidentalis* (pumpkin leaf) were collected from a farm in Uyo and washed several times with water to remove the dust particles. They were sun dried to remove the residual moisture and ground to form powder. Then plant extract was prepared by mixing 1% of plant extract in deionized water in a 250 ml of conical flask. Then, the extract was centrifuged for 30 min at 5000 rpm. The supernatant was separated with Whatman filter paper. Then the resultant solution was used for the reduction of silver ions (Ag^{+}) to silver nanoparticles (Ag°).

Synthesis of silver nanoparticles

Preparation of 1% w/v of silver nitrate solution

Silver nitrate solution (1% w/v) was prepared by dissolving 5.0 g of silver nitrate in distilled water and making the volume to 500 ml.

Preparation of polymer solution

Xanthan gum suspension (0.25, 0.50, 0.75 and 1.0% w/v) was prepared by dissolving 0.25, 0.5, 0.75, and 1.0 g of Xanthan gum in 100 mL of distilled water. These served as stabilizing agents in the nanoparticle synthesis.

Preparation of silver nanoparticles

To each of the polymer suspension, 2.5 ml of silver nitrate solution was added in drops over a period of 30 s under constant stirring using a magnetic stirrer assembly. This was followed by incorporation of 10 ml of reducing agent (freshly prepared edible plant extract). The composition of the silver nanoparticles is shown in Table 1.

UV Vis spectroscopy

The optical property of AgNPs was determined by UV-Vis spectrophotometer, UNICO 2100, China. UV-Vis spectrophotometer allows identification, characterization and analysis of metallic nanoparticles. In general, 200 to 800 nm light wavelength is used for the characterization.

Antimicrobial studies

Agar dilution method was used to determine the antimicrobial activities of the silver nanoparticle against *S. aures, Bacillus subtilis, Pseudomonas aeruginosa,* and *Escherichia coli.* Microbes were pipetted and dropped on 3 batches of petri dishes (12 plates) already labeled with respect to the nanoparticles and their concentrations. 20 ml of Mackonkey agar (HiMedia) was swirled with the cultures. Sterile Cork borer of 4 mm diameter was used to bore four holes in each plate (three holes for nanoparticles' concentrations 0.05, 0.10, and 0.15% w/v and one hole for the control of which an antibacterial standard drug-Erythromycin were used). The silver nanoparticles were placed in each hole of the agar plate and incubated at 37°C for 24 h. Based on inhibition zones around the hole, the antimicrobial activities were measured saturated with plant extract synthesized silver nanoparticle. The results are shown in Table 3.

RESULTS AND DISCUSSION

The results for the characterization of synthesized

Table 1. Composition of Silver nanoparticles.

Batches	Xanthan gum (g)	Distilled water (ml)	$AgNO_3$ (ml)	Reducing agent (ml)
0.25% w/v VA	0.2 5	100	2.5	10
0.5% w/v VA	0.5	100	2.5	10
0.75% w/v VA	0.75	100	2.5	10
1.0% w/v VA	1.0	100	2.5	10
0.25% w/v TO	0.25	100	2.5	10
0.5% w/v TO	0.5	100	2.5	10
0.75% w/v TO	0.75	100	2.5	10
1.0% w/v TO	1.0	100	2.5	10
0.25% w/v LA	0.25	100	2.5	10
0.5% w/v LA	0.5	100	2.5	10
0.75% w/v LA	0.75	100	2.5	10
1.0% w/v LA	1.0	100	2.5	10

VA, TO and LA stands for, *Vernonia amygdalina*, *Telfaria occidentalis* and *Lasianthera africana,* respectively.

Table 2. SPR bands of Silver nanoparticles characterization.

Batches	Distilled water (ml)	$AgNO_3$ (ml)	Reducing agent (ml)	Colour change	SPR peak (nm)
0.25% w/v VA	100	2.5	10	Reddish brown	451
0.5% w/v VA	100	2.5	10	Reddish brown	451
0.75% w/v VA	100	2.5	10	Reddish brown	451
1.0% w/v VA	100	2.5	10	Reddish brown	451
0.25% w/v TO	100	2.5	10	Reddish brown	452
0.5% w/v TO	100	2.5	10	Reddish brown	451
0.75% w/v TO	100	2.5	10	Reddish brown	416
1.0% w/v TO	100	2.5	10	Reddish brown	411
0.25% w/v LA	100	2.5	10	Reddish brown	371
0.5% w/v LA	100	2.5	10	Reddish brown	371
0.75% w/v LA	100	2.5	10	Reddish brown	372
1.0% w/v LA	100	2.5	10	Reddish brown	371

VA, TO and LA stands for, *V. amygdalina*, *T. occidentalis* and *L. africana,* respectively.

Table 3. Antimicrobial activities of silver nanoparticles.

Microorganism	Zone of inhibition (cm)			
	Standard drug (Erythromycin)	*V. amygdalina*	*T. occindentalis*	*L. africana*
E. coli	3.5	1.3	1.4	0.15
S. aureus	1.5	1.2	1.5	1.6
P. aeruginosa	2.5	1.5	1.3	1.4
B. subtilis	2.6	1.5	1.3	1.8

nanoparticles are shown in Table 2. The results for the determination of optimized batches of antimicrobial activities of synthesized silver nanoparticles are shown in Table 3.

Antimicrobial studies

The antimicrobial activity of silver nanoparticles was carried out against both Gram positive and Gram negative bacteria. The synthesized silver nanoparticles exhibited good antibacterial activity against both Gram negative and Gram positive bacteria. Based on the zones of inhibition produced (Table 3), *E. coli* was most sensitive to *L. Africana* (inhibition zone diameter = 1.5 cm) and least sensitive to *T. occidentalis* (inhibition zone diameter = 1.3 cm). *B. subtilis* was also least sensitive to *T. occidentalis* (inhibition zone diameter = 1.3 cm) and

most sensitive to *L. africana* (inhibition zone diameter = 1.8 cm). A similar trend of sensitivity was observed with *P. aeruginosa.* However, with *Staphylococcus aureus*, the sensitivity pattern was slightly different. The microorganism was most sensitive to *L. africana* (inhibition zone diameter = 1.6 cm) but least sensitive to *V. amygdalina* (inhibition zone diameter = 1.2 cm). Among the different vegetables used in the study, *L. africana* appeared to have the broadest antimicrobial activity.

Silver nanoparticles are widely known for their antimicrobial properties. The widespread cases of multidrug resistant bacteria against the standard antibiotics have led scientists to potentially incorporate AgNPs and other nanomaterials as ingredient to enhance the antibiotic efficacy (Ali et al., 2016). In some cases, all the microbes were all eliminated (Sathishkumar et al., 2009). There have been several proposed mechanisms on how AgNPs work as antibacterial, although the exact mechanism is still unknown. Several reports including Kumar and Münstedt (2005) suggested that the AgNPs could produce Ag ions which will damage the cell membrane, interrupt the metabolic activity, and subsequently lead to denaturation of protein and finally cell death. AgNPs could also produce reactive oxygen species (ROS) such as singlet oxygen $^1O_2$, hydroxyl radical ·OH, and peroxide radical R-O-O• which are harmful to the bacteria (Carlson et al., 2008).

Colour change

Reduction of silver ions into silver nanoparticles during exposure to plant extracts was observed as a result of the colour change. The colour change was due to the surface plasmon resonance (SPR) phenomenon. The metal nanoparticles have free electrons, giving the SPR absorption band, due to the combined vibration of electrons of metal nanoparticles in resonance with light wave. Silver nanoparticles synthesized from plants extracts have been observed to exhibit brownish colour in aqueous solution due to SPR (Logeswari et al., 2015).

UV Vis spectroscopy

The sharp bands of silver nanoparticles were observed around 451 nm in case of *V. amygdalina* for all four concentrations, whereas the bands for *L. africana* were observed around 371 nm (0.25 g), 371 nm (0.75 g), and 371 nm (1.0 g). For *T. occidentalis*, the bands were observed at 452 nm (0.25 g), 451 nm (0.5 g), 416 nm (0.75 g), and 411 nm (1.0 g). From different literature, it was found that the silver nanoparticles show SPR peak at around 420 to 450 nm (Rao and Tang, 2017; Ali et al., 2016). From these studies, the SPR peak for *T. occidentalis* was found at 451 nm and the SPR peak for *V. amygdalina* was found at 451 nm, whereas for *L. africana*, it was found at 371 nm. These results are similar to the SPR peaks observed by Jackson et al. (2016). *T. occidentalis* and *V. amygdalina* leaf extracts seem to have more potential to reduce Ag ions into Ag nanoparticles than *L. africana*. The intensity of absorption peak increases with time. This characteristic colour variation is due to the excitation of the SPR in the metal nanoparticles. The reduction of the metal ions occur fairly rapidly; more than 90% of reduction of Ag+ ions was complete within 4 h after addition of the metal ions to the plant extract. The metal particles were observed to be stable in solution even 4 weeks after their synthesis. There was no visible change in colour and the UV-Vis peaks of the nanoparticle solutions with time.

Conclusion

The rapid biological synthesis of silver nanoparticles using bitter leaf (*V. amygdalina*), editan leaf (*L. africana*), and pumpkin leaf (*T. occidentalis*) extract provides environmental friendly, simple and efficient route for synthesis. The change in colour from yellow to reddish brown is the characteristic of silver nanoparticles. SPR characteristic peak for the synthesized nanoparticles gave values from 371 to 452 nm which confirmed the formation of silver nanoparticles. Nanoparticles synthesized from *V. amygdalina* and *T. occidentalis* have similar ($P<0.05$) peaks for the SPR. Nanoparticles synthesized from *L. africana* had at least SPR (371 nm). After nine months of storage at room temperature and at 4°C, the SPR peak and colour of nanoparticles remain unchanged.

These edible plants used in the synthesis are readily available, affordable, non-toxic and biocompatible. They are generally regarded as safe (GRAS). The antimicrobial activity of these nanoparticles was studied against *E. coli, S. aureus, P. aeruginosa* and *B. subtilis.* They have the satisfactory inhibitions against the four mentioned microorganisms. Among the different vegetables used in the study, nanoparticles synthesized from *L. africana* appeared to have the highest antimicrobial activity.

CONFLICT OF INTERESTS

The authors have not declared any conflict of interests.

ACKNOWLEDGEMENT

The authors are grateful to Tertiary education Trust Fund (TETFund), Nigeria for supporting the work..

REFERENCES

Ali ZA, Yahya IR, Sekaran SD, Puteh R (2016). Green Synthesis of Silver Nanoparticles Using Apple Extract and Its Antibacterial

Properties. Advances in Materials Science and Engineering Volume 2016, Article ID 4102196, 6 pages.
Carlson C, Hussein SM, Schrand AM (2008). Unique cellular interaction of silver nanoparticles: size-dependent generation of reactive oxygen species. The journal of physical chemistry B 112(43):13608-13619.
Ganesan V, ArunaDevi J, Astalakshmi A, Nima P, Thangaraja A (2013a). Eco-friendly synthesis of silver nanoparticles using a sea weed, *Kappaphycus alavarezii.* International Journal of Nanotechnology 2(5):559-563.
Ganesan V, Astalalshmi A, Nima P, Arunkumar C (2013b). Synthesis and characterization of silver nanoparticles using Merremia *tridentate* (L). Hall, F. International Journal of Current Science 6:87-93.
Jackson TC, Agboke A, Jackson I, Ekpuk E (2016). Biosynthesis of Silver nanoparticles using M*urraya Koenigii* and Acacia Gum. International Journal of Research in Pharmacy and Biosciences 3(2):29-32.
Khan M, Khan M, Adil SF, Tahir MN, Tremel W, Alkhathlan HZ, Al-Warthan A, Siddiqui MRH (2013). Green synthesis of silver nanoparticles mediated by *Pulicaria glutinosa* extract. International journal of nanomedicine 8:1507-1516.
Korbekandi HIS, Abbasi S (2009). Production of nanoparticles using organisms. Critical Reviews in Biotechnology 29:279-306.
Kumar P, Suranjit P, Darshit P, Patel A, Dalwadi P, Prasad R, Patel P, Selvaraj K, Prasad S (2011). Biogenic synthesis of silver nanoparticles using Nicotiana tobaccum leaf extract and study of their antibacterial effect. African Journal of Biotechnology 10(41):8122-8130.
Kumar R, Münstedt H (2005). Silver ion release from antimicrobial polyamide/silver composites. Biomaterials 26(14):2081-2088.
Logeswari P, Silambarasan S, Abraham J (2015). Synthesis of Silver nanoparticles using plants extracts and analysis of their antimicrobial property. Journal of Saudi Chemical Society 19:311-317.
Ndikau M, Noah NM, Andala DM, Masika E (2017). Green Synthesis and Characterization of Silver Nanoparticles Using *Citrullus lanatus* Fruit Rind Extract. International journal of analytical chemistry Article ID 8108504, 9 pages.
Rao B, Tang RC (2017). Green synthesis of silver nanoparticles with antibacterial activities using aqueous *Eriobotrya japonica* leaf extract. Advances in Natural Sciences: Nanoscience and Nanotechnology 8(1):015014.
Roy S, Das TK (2015). Plant mediated green synthesis of Silver nanoparticles. A Review. International Journal of Plant Biology and Research. 3(3):1044-1055.
Sachin S, Anupama P, Meenal K (2012). Biosynthesis of silver nanoparticles by marine bacterium, *Idiomarine Sp.* PR – 58-5. Bulletin of Materials Science 35(7):1201-1205.
Sathishkumar M, Sneha K, Won SW, Cho CW, Kim S, Yun YS (2009). *Cinnamon zeylanicum* bark extract and powder mediated green synthesis of nano-crystalline silver particles and its bactericidal activity. Colloids and Surfaces B: Biointerfaces 73(2):332-338.
Xin Y, Qingbiao LI, Huixuan W, Jiale H, Liqin L, Wenta W, Daohua S, Yuanbo S, James B, Luwei H, Yuanpeg W, Ning H, Lishan J (2010). Green synthesis of palladium nanoparticles using broth of Cinnamomum camphora leaf. Journal of Nanoparticle Research 12:1589-1598.
Yang WT, Li H, Gong Y, Chen WY, Gaidau C (2011). Preparation of silver nanoparticles of enhanced antibacterial effect with benzalkonium bromide. Journal of Optoelectronics and Advanced Materials 13(6):661-665.

Vol. 17(24), pp. 753-759, 13 June, 2018
DOI: 10.5897/AJB2018.16507
Article Number: 9DF23F857422
ISSN: 1684-5315

http://www.academicjournals.org/AJB

African Journal of Biotechnology

Full Length Research Paper

Identification and genetic diversity of Jordanian potato soft rot isolates, *Pectobacterium carotovorum* subspecies *carotovorum* (DYE 1969)

Ibtihal Abu-Obeid[1*], Hamed Khlaif[2] and Nida Salem[2]

[1]Plant Protection Directorate, National Agricultural Research Center (NARC), Jordan.
[2]Plant Protection Department, Faculty of Agriculture, the University of Jordan, Jordan.

Received 2 May, 2018; Accepted 5 June, 2018

Bacterial soft rot disease is one of the most important factors affecting potato production in Jordan. Based on biochemical and physiological analyses, Jordanian isolates of soft rot from potato were identified as *Pectobacterium carotovorum* subspecies *carotovorum* (DYE 1969). Phylogenetic analysis using *pmrA* gene sequence data showed that isolates from different regions were closely related to each other, whereas little genetic diversity was observed between these isolates. A DNA marker was developed from nucleotide sequences of the *pmrA* gene and a 318 bp fragment was polymerase chain reaction (PCR) amplified specifically from *P. carotovorum* subspecies *carotovorum* isolates, which could be used for detection of the disease in potato tubers.

Key words: Potato soft rot, *Solanum tuberosum*, genetic diversity, *pmr*A gene, *Pectobacterium carotovorum* subspecies *carotovorum*, Jordan.

INTRODUCTION

Potato (*Solanum tuberosum* L.) is one of the most common and important vegetable crops in Jordan, used for both consumption and export. During 2016, area planted with potato was 508600 hectares with production of 15858000 kg (Anonymous, 2016).

Bacterial soft rot disease is commonly found in potato growing regions worldwide (Perombelon, 2002; Czajkowski et al., 2009). Several studies have shown that the soft rot causal agents are too divergent to be included in one clade (Knwon et al., 1997; Hauben et al., 1998). The new classification grouped the genus *Erwinia* into *Pectobacterium* (formally *Erwinia carotovora*) and *Dickeya* spp., according to the differences of pectolytic enzymes secreted through type II secretion system. Two species, *Dickeya chrysanthmi* and *Pectobacterium carotovorum* are particularly damaging to potato production (Toth et al., 2001; Czajkowski et al., 2009). *P. carotovorum* is a highly diverse species and is currently divided into five subspecies: a*trosepticum*, *betavasculorum*, *carotovorum*, *odoriferum* and *wasabiae* (Hauben et al., 1998) with subspecies *carotovorum* and *atrosepticum* causing rotting of potato during vegetative growth and in stored tubers.

Control of bacterial diseases depends on the accurate

*Corresponding author. E-mail: ibtihal@narc.gov.jo.

detection and identification of the causal agent. Although, diagnosis of bacterial diseases based on symptoms is simple, symptoms are not always specific and can be confused with other biotic or abiotic factors. For preventive control measures, detection of the causal agent in symptomless plant material is necessary, but can be difficult, because the pathogen may be present in low population densities and in uneven distribution in the infected plants (Palacio-Bielsa et al., 2009). However, the diagnosis of the disease is not always related to field inspection, so, it is important to detect the pathogen in seed potato tubers before distribution to farmers in order to prevent spreading the disease. Efficient, low cost detection and identification methods are essential to investigate the ecology and pathogenesis of soft rot Enterobacteriaceae as well as in seed certification programmes (Czajkowski et al., 2014).

In a review by Czajkowski et al. (2014), more than 30 methods have been employed to detect, identify and differentiate soft rot causal agents to species and subspecies levels; including biochemical characters, serology and molecular techniques. Within the past 30 years, there has been a shift from microbiological and serological methods to molecular approaches (Palacio-Bielsa et al., 2009; Czajkowiski et al., 2014). DNA markers have been used for the rapid detection of different strains of *P. carotovorum* subspecies *carotovorum* (*Pcc*) (Kang et al., 2003; Zhu et al., 2010; Rahmanifer et al., 2012; Azadmanesh et al., 2013). DNA sequence analysis of gene *pmr*A, which is linked to pathogenicity (response regulator), was used to evaluate the relationship among *Pcc* isolates collected from different regions of Morocco and results were equivalent to enterobacterial repetitive intergenic consensus-polymerase chain reaction (ERIC-PCR) and 16S rDNA sequencing (Kettani-Halabi et al., 2013).

In Jordan, *Erwinia carotovora* subsp. *carotovora*, which is recently known as Pcc, was identified as the causal agent of soft rot disease of vegetables, its detection and identification was carried out through traditional techniques. The pathogen infects and causes disease on a wide variety of hosts belonging to different families of vegetables either in field and storage in different areas including, Jordan Valley and Uplands. Soft rot of potatoes is a tuber borne disease where the contaminated mother tubers are reported to be the main source of inoculum. However, this bacterium was found to survive in the soil with population trends varying with the fluctuation in soil temperature (Rajeh and Khlaif, 2000).

Traditional techniques used for detection and identification of the causal agents are time consuming and relatively insensitive. Therefore, there is an urgent need for a sensitive and highly specific technique for rapid detection and identification of Pcc.

In this study, the detection, identification and genetic diversity of Jordanian isolates of *P. carotovorum* subspecies *carotovorum* were evaluated based on *pmrA* gene sequencing analysis.

MATERIALS AND METHODS

Samples collections and bacterial isolation

Samples including stem and tubers suspected to be infected with soft rot were randomly collected throughout potato growing areas in Jordan during the growing seasons, fall and spring seasons and from storage facilities from different potato growing areas in Jordan.

Twenty potato growing regions and nine storage sites were surveyed and representative potato samples were collected from each site. Logan's and nutrient agar media were used for bacterial isolation (Fahy and Parsley, 1980; Schaad et al., 2001). The *P. carotovorum* subspecies *carotovorum* (Pcc) reference culture NCPPB312 was obtained from Food and Environment Research Agency, United Kingdom to identify *Pcc* isolates.

Biochemical and physiological tests

The 205 *Pcc* isolates were evaluated for oxidase and catalase reactions, potato soft rot, oxidative fermentative, ability to grow at 37°C, sodium chloride tolerance, reducing substances from sucrose, urease production and acid production from carbohydrates utilized as carbon source as described by Schaad et al. (2005) for characterization of the isolates.

Genomic DNA extraction from bacterial cultures

Pure bacterial cultures grown on NA media at 37°C for 24 h were used for DNA extraction. Genomic DNA was extracted using the DNeasy Blood and Tissue Kit (Qiagen, Valancia, CA) according to the manufacturer's instruction. DNA was quantified and stored at -20°C for further analysis.

Characterization of isolates with *pmr*A marker

The isolates were subjected to PCR amplification using *pmr*A primer set: F0145: TACCCTGCAGATGAAATTATTGATT-GTTGAAGA; E2477: TACCAAGCTTTGGTTGTTCCCCTTTGGTCA (Kettani-Halabi et al., 2013). Primers were designed based on the sequence of *pmr*A *gene* in *Erwinia* species.

DNA amplification were performed in a BIORAD T100™ thermal cycler (BioRad, Hercules, CA) using the following protocols. PCR amplification was conducted in a 25 µl reaction containing 5.0 µl Crimson Taq buffer (5X), 1.1 µl $MgCl_2$ (25 mM), 0.5 µl of dNTPs (10 mM), 1.25 µl of each primer (10 µM), 0.13 µl of Taq polymerase (5U/µl) and 2 µl of the template DNA where its concentrations ranged between 450 and 600 ng/µl. The reaction involved initial denaturation (94°C for 3 min) followed by 32 cycles of denaturation (94°C for 1 min), annealing (47°C for 1 min), extension (72°C for 1 min) and final extension (72°C for 7 min). The amplified products were electrophoretically separated in 1.5% (w/v) agarose gel at 110 V for 35 min in TBE buffer and visualized with UV light after staining in a solution of ethidium bromide (0.5 µg/mL).

DNA sequencing of PCR amplification products

Samples were chosen after showing the specific bands. Taken into consideration resembling of different potato growing regions, bulk PCR amplification was conducted as described above for *Pcc*

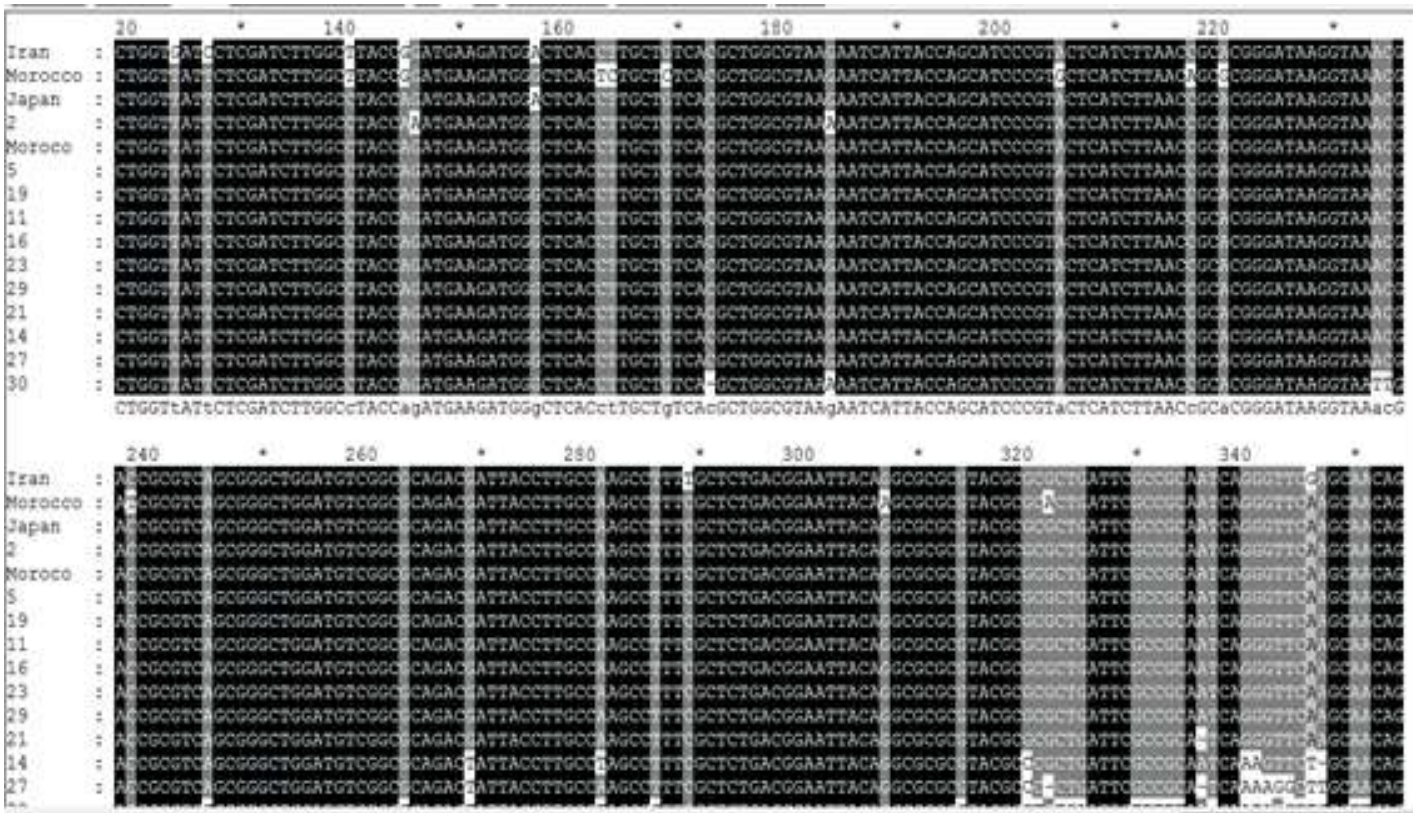

Figure 1. pmrA nucleotides sequences alignment used to design primers specific for PCR amplification of *Pectobacterium carotovorum* subsp. *carotovorum* Jo-isolates Q; 16, 27, 30, 19, 14, 21, 29, 23, A; 11, 2, 5 and Pcc reference strains; Pcc strain P603AH1 (Acc. no. JQ278721.1) and Pcc strain P116C2 (Acc. no. JQ278749.1) from Morocco; Pcc, Iran strain Irca3 (Acc. no. KJ634063.1) and Pcc Japan strain (Acc. no. AB447882.1).

isolates. DNA bands were excised from agarose gels and purified using Wizard SV Gel and PCR Clean Up System (Promega) according to the manufacturer's instructions.

DNA fragments were ligated into the pGEM-T Easy Vector (Promega) according to the manufacturer's instructions. Ligated products were transformed into JM109 high efficiency competent cells. Five recombinant colonies (white colonies), were selected for each reaction and grown in 4 mL LB broth containing ampicillin (100 µg/ml), at 37°C overnight with shaking at 200 rpm. Plasmid DNA was isolated from cultures using the Pure Yield Plasmid Miniprep Kit. Clones were tested for inserts and fragment size and two clones, from each *Pcc* isolate were sent for sequencing to Macrogen (Seoul, Rep. of Korea) and sequenced from both directions using SP6 and T7 primers.

Sequence analysis

The DNA sequence data were analyzed and homology search was performed using Basic Local Alignment Searching Tool (BLAST) at NCBI (http://blast.ncbi.nlm.nih.gov/Blast.cgi). Multiple alignments were conducted using the ClustalX (Thompson et al., 1997). The sequences were then analyzed using GenDoc program from MEGA (Kumar et al., 2001).

Phylogenetic analysis

Evolutionary tree was reconstructed using the Neighbor-Joining (NJ) program of MEGA (Kumar et al., 2001). The stability of relationships was assessed by performing bootstrap analyses of the Neighbor-Joining with a 1000 replicate bootstrap search.

Primers design

Comparisons of sequences of *pmr*A and other sequences of reference strains published in the GenBank were performed (Figure 1) and new specific primers were designed on the basis of similarities between *Pcc* Jo-isolates. Primer was designed using Primer3 software available at NCBI. Both specificity and sensitivity for set of primers were determined.

In order to assess the specificity of the designed primers, PCR was carried out for different isolates confirmed earlier as *Pcc* together with isolates belonging to other bacterial genera.

To assess the sensitivity of the designed primers, serial dilutions of different bacterial DNA extracts were prepared in NFW from 1×10^{-1} to 1×10^{-7} diluted from 100 ng DNA as well as DNA without dilution, then 2 µl aliquots were directly used as templates for PCR reaction using set of primers.

RESULTS

Two hundred and five rotted potato samples suspected to be infected with soft rot disease were collected from fields and storage throughout potato growing areas in

Table 1. Locations, sampling date and number of samples collected.

Region	Location	Sampling date	Number of samples collected
Amman	Commercial Stores	26/07/2015	15
AR Ramtha	Torrah/Hallan Way	10/06/2014	15
	Torrah/Tanqeeh Station	16/04/2014	16
Jordan Valley	Ashshuna Al Janoubiyya /Wadi Al Abiad	20/01/2014	3
	Deir Alla	15/01/2014	5
	Deir Alla Station	08/04/2014	6
	Ghor Kabed	26/03/2014	25
	Karameh	29/01/2014	8
	North Ghor/Al Sleakhat	20/11/2013	5
	Sharhabeel	16/02/2014	25
Ma'an	Modawwarah	23/01/2014	5
	Modawwarah	29/05/2014	8
	Al Quwayra	08/05/2014	6
Madaba	Al Ariesh	03/07/2014	4
	Jrainah	13/11/2013	14
	Samek	23/04/2014	6
Mafraq	Mghayyer serhan	29/06/2014	2
	Sama serhan	15/01/2014	9
	Sama serhan	26/07/2015	20
	Thoghret El-Jobb	29/06/2014	8
Total number of samples			205

Jordan during summer, autumn and winter seasons, from November, 2013 to July, 2015 in 20 locations (Table 1).

Biochemical and physiological tests

Bacterial isolates were found to be oxidase negative, catalase positive, fermentation of glucose positive, rotting induced on inoculated potato slices, urease enzyme producing, develop growth on nutrient agar plates incubated at 37±2°C and on 5% NaCl. Also, all isolates were able to oxidize the alcoholic sugar and discharge it in the media to acidic reaction and were not able to reduce substances from sucrose. The reactions of the tested bacterial isolates to the different biochemical, physiological and nutritional tests were identical with the results of the same tests conducted for the reference bacterial culture of *Pcc* isolate NCPPB312.

Detection of *Pcc* using (PCR) with *pmr*A primer set

The DNA extracts of different isolates biochemically identified as *Pcc* were of good quality and quantity; distinctive bands were detected when DNA extracts were ran in 1.0% agarose gel. Furthermore, the spectrophotometer readings indicated that the DNA concentrations ranged between 450 and 600 ng/µl and the 260/280 ratio ranged between 1.8 and 2.0. Bacterial isolates showed band of about 666 bp (Figure 2) when tested using the specific set of primers *pmr*A (F0145/E2477).

Sequencing analysis

Maximum nucleotide similarity (BLASTn) with closely related species/subspecies ranged from 91 to 100% with *Pcc* strain P603AH1 (Acc. no. JQ278721.1) from Morocco. Similar results were obtained with maximum amino acid similarity (BLASTx).

Phylogenetic analysis

Most of the isolates from Mafraq (Jo-Q16, 19 and 23) and Amman (Jo-A5 and 11) formed a single cluster together with strains from Morocco, Iran and Japan with a

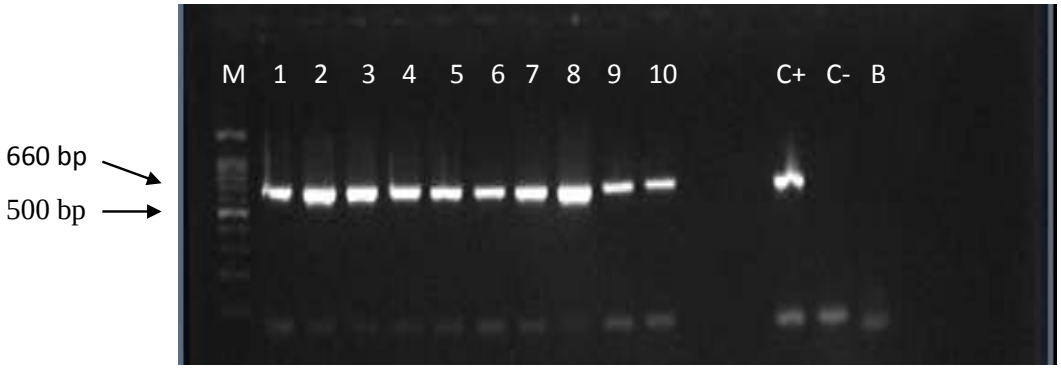

Figure 2. Agarose gel electrophoresis for PCR-amplified DNA of *Pectobacterium carotovorum* subsp. *carotovorum* isolates using *pmr*A primers set with the expected amplified product of 660 bp. Lane M represents Ladder 100 bp (GeneDirex). Lanes 1- 10, isolates Jo-Q16, Q19, A11, A2, Q14, Q21, Q29, A5, Q23 and Q27, respectively. Lanes C+, positive control (reference isolate NCPPB312), C-: Negative control isolate *Escherichia coli* and B: Buffer (Abu-Obeid et al., 2018).

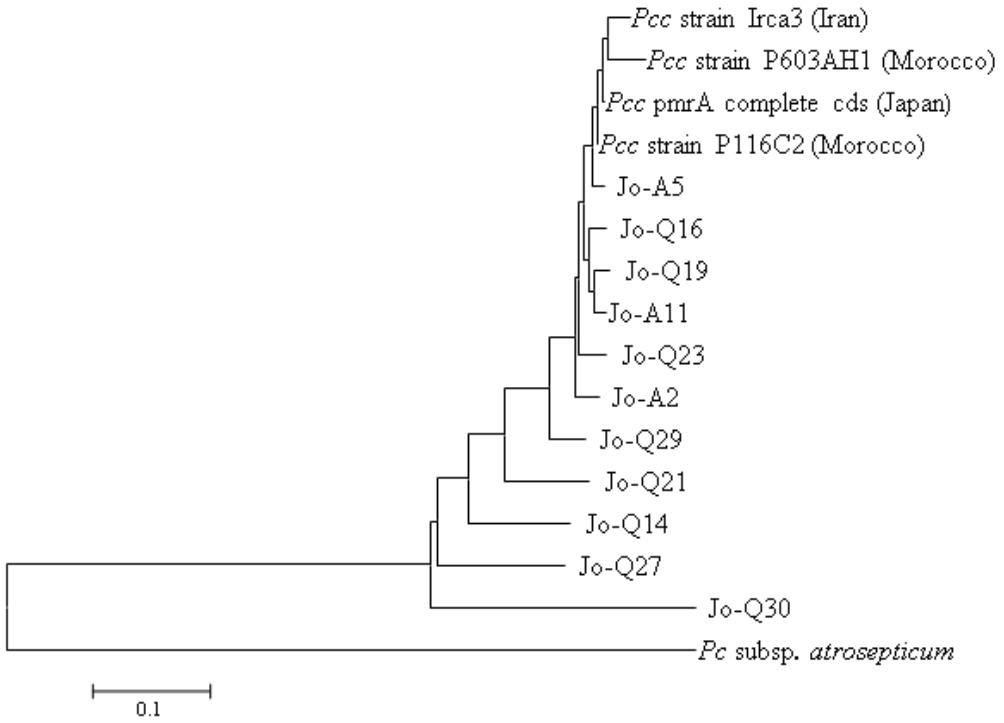

Figure 3. Phylogenetic analysis of nucleotide sequences of *Pectobacterium carotovorum* subsp. *carotovorum* Jo-isolates and reference strains based on *pmr*A partial gene sequences. The generation of the tree was conducted in MEGA program. The branching pattern was generated by the Neighbor-Joining method; stability of the tree was assessed by 1000 bootstrap replication. *Pectobacterium carotovorum* subsp. *atrosepticum* (Acc. no. AY209016.1) was used as out group.

bootstrap value of 92%, while the rest isolates clustered individually but were close to each other. Q30 isolate formed a single cluster, on the other hand, Q30 had lower similarity but higher E-value than the rest *Pcc* Jo-isolates which formed a single cluster clearly differentiating them from out group *P. carotovorum* subsp. *atrosepticum* (*Pca*) (Acc. no. AY209016.1); the results support the classification of *Pcc* isolates as subspecies distinct from *Pca* (Figure 3).

PCR marker development

The new designed primer Jo-*pmr*A/For. GTCACGAAGG-

Figure 4. Agarose gel electrophoresis for PCR-amplified DNA for *Pectobacterium carotovorum* subsp. *carotovorum* isolates using designed *pmr*A primers set with the expected product size of 318 bp. Lane M represents Ladder 100 bp (GeneDirex). Lanes 1-10: isolates Jo-Q16, Q19, A11, A2, Q14, Q29, A5, Q30, Q23 and Q27; lanes 11 and 12: *Bacillus* spp. and *Listeria* spp., respectively. Lanes C+: Positive control (reference isolate NCPPB312) and B: Buffer.

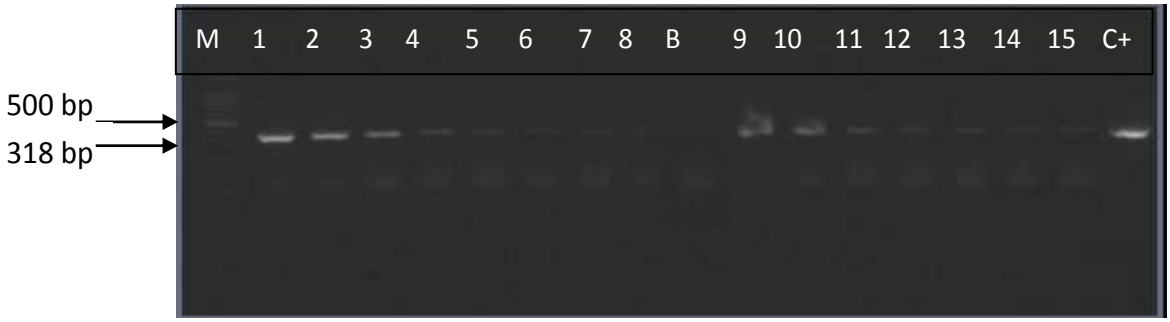

Figure 5. Agarose gel electrophoresis for PCR-amplified DNA for *Pectobacterium carotovorum* subsp. *carotovorum* Jo-isolates using designed *pmr*A primers set with the expected product size of 318 bp. Lane M represents Ladder 100 bp (GeneDirex). Lanes 1-8, isolates Jo-Q2 un-diluted, serial dilutions from 1×10^{-1} up to 10^{-7}; lanes 9-15, isolates Jo-Q21 un-diluted, serial dilutions from 1×10^{-1} up to 10^{-6}, respectively. Lanes C+, positive control (reference isolate NCPP312) and B: Buffer.

TTATGCCTGC, Jo-*pmr*A/Rev. AGCACCACTGGCTTGT-CATC, was used to test PCR specificity and sensitivity to *Pcc* Jo-isolates; length of the primer was 20 bp, melting temperature (Tm) ranged from 56.3 to 57.9°C and GC ratio was 55% with an expected product size of 318 bp.

The marker was specific for detection of *Pcc* Jo-isolates: Jo-Q16, Q19, A11, A2, Q14, Q29, A5, Q30, Q23 and Q27, where it produced PCR product of 318 bp and no bands were observed when tested with other bacterial genera: *Bacillus* spp. and *Listeria* spp. (Figure 4). The marker was sensitive for detection of DNA concentration up to 1.0×10^{-4} ng/µl (Figure 5).

DISCUSSION

Seed potatoes planted in Jordan are imported each year from different countries, distributed worldwide in addition to local production of many varieties. Potato tuber yield losses have increased due to soft rot which has spread in potato cultivation regions including Amman, AR Ramtha, Jordan Valley, Ma'an, Madaba and Mafraq.

Using specific primers for *pmr*A gene, isolates produced a 666 bp; results confirmed these isolates as *Pcc*. Furthermore, the phylogenetic analysis showed that all isolates clustered together with different *Pcc* reference strains available in the GenBank. The *Pcc* Jo-isolates were strongly differentiated from other *Pectobacterium* responsible for disease in potato including *Pca*.

Kettani-Halabi et al. (2013) indicated that *pmr*A sequence analysis was a reliable tool for detection and identification of *Pcc* and to determine genetic diversity. The *Pcc* Jo-isolates from different regions did not cluster according to locations and this could be attributed to the fact that potato seeds in Jordan are mainly from one source.

Terrta et al. (2011) did not observe any correlation between ERIC-PCR analysis, geographical areas and year when they studied the genetic distribution and epidemiological typing of *Pcc*.

Conclusions

Amplification of a specific region and using specific set of primer is a sensitive method for detecting *Pcc.* Little genetic diversity was found among isolates obtained from different regions and similarity was found between them.

CONFLICT OF INTERESTS

The authors have not declared any conflict of interests.

REFERENCES

Anonymous (2016). The Hashemite Kingdom of Jordan. Ministry of Agriculture Statistical Year Book.

Abu-Obeid I, Khlaif H, Salem N (2018). Comparison of Different Sets of Primers Used in Detection and Identification of Potato Soft Rot *Pectobacterium carotovorum* subsp. *carotovorum* (DYE1969). Asian Journal of Research in Crop Science 1(1):1-12.

Azadmanesh S, Marefat A, Azadmanesh K (2013). Detection of Pectobacteria causal agents of potato soft rot in north western provinces of Iran (Electronic Version). Journal of Plant Pathology and Microbiology 4:1.

Czajkowski R, Grzegorz G, van der Wolf J (2009). Distribution of Dickeya spp. and *Pectobacterium carotovorum* ssp. carotovorum in naturally infected seed potatoes. European Journal of Plant Pathology 125:263-275.

Czajkowski R, Perombelon M, Jafra S, Lojkowaska E, Prtrykus M. van der Wolf J, Sledz W (2014), Detection, identification and differentiation of Pectobacterium and Dickeya species causing potato black leg and tuber soft rot: a review. Annals of Applied Biology 166: 18-28.

Fahy P, Parsley G (1983). Plant Bacterial Diseases. (1st ed.), Sydney: Academic Press

Hauben L, Moore E, Vauterin L, Steenackers M, Mergaert J, Verdonck L, Swings J (1998). Phylogenetic position of phytopathogens within the Enterobacteriaceae. Systemic Applied Microbiology 21(3):384-397.

Kang H, Knwon S, Go S (2003). PCR-based specific and sensitive detection of *Pectobacterium carotovorum* ssp. carotovorum by primers generated from URP-PCR finger printing-derived polymorphic band. Plant Pathology 52:127-133.

Kettani-Halabi M, Tera T, Amdan M, El Fahime E, Bouteau F, Mustapha M (2013). An easy, simple inexpensive test for the specific detection of *Pectobacterium carotovorum* ssp. carotovorum based on sequence analysis of the pmrA gene. BMC Microbiology 13:176-182.

Kumar S, Tamura K, Jakobsen IB, Nei M (2001). MEGA2: Molecular evolutionary genetics analysis software. Bioinformatics Applied Note 17:1244-1245.

Palacio-Bielsa A, Cambra M, Lopez M (2009). PCR detection and identification of plant pathogenic bacteria: updated review of protocols (1989-2007). Journal of Plant Pathology 91(2):249-297.

Perombelon M (2002). Potato diseases caused by soft rot erwinias: an overview of pathogenesis. Plant Pathology 51:1-12.

Rahmanifer B, Hassnzadeh N, Razmi J, Ghasemi A (2012). Genetic diversity of Iranian potato soft rot bacteria based on polymerase chain reaction-restriction fragment length polymorphism (PCR-RFLP) analysis. African Journal of Biotechnology 11(6):1314-1320.

Rajeh O, Khlaif H (2000). Soft rot disease of vegetables in Jordan: host range, reaction of some potato cultivars to the identification and effect of planting date. Dirasat, Agricultural Sciences 27(2):149-157.

Schaad N, Jones J, Chun W (2005), Laboratory Guide for Identification of Plant Pathogenic Bacteria (3rd ed.), Minnesota: APS, St. Paul.

Thompson JD, Gibson TJ, Plewniak F, Jeanmougin F, Higgins DG (1997). The CLUSTALX windows interface; flexible strategies for multiple sequence alignment aided by quality analysis tools. Nucleic Acids Research 25:4876-4882.

Toth I, Avrova A, Hyman L (2001). Rapid identification and differentiation of the soft rot Erwinias by 16S-23S intergenic transcribed spacer-PCR and Restriction Fragment Length Polymorphism Analyses. Applied Environmental Microbiology 67:4070-4076.

Terrta M, Azelmat S, M'hand R, Achbani E, Barakate M, Bouteau F, Ennaji M (2011). Molecular typing of *Pectobacterium carotovorum* isolated from potato tuber soft rot in Morocco. Annals Microbiology 47:1411-1417.

Zhu I, Xie H, Chen S, Ma R (2010), Rapid isolation, identification and phylogenetic analysis of *Pectobacterium carotovorum* ssp. Journal of Plant Pathology 92(2):479-483.

Vol. 17(24), pp. 760-766, 13 June, 2018
DOI: 10.5897/AJB2018.16427
Article Number: 02E067157424
ISSN: 1684-5315

http://www.academicjournals.org/AJB

ACADEMIC JOURNALS
expand your knowledge

African Journal of Biotechnology

Short Communication

Studies on enhanced African black soap from *Theobroma cacao* (cocoa) and *Elaeis guineensis* (palm kernel oil)

Adebomi A. Ikotun[1*], Esther O. Faboro[1], Adejoke S. Kolade[1] and Abimbola A. Owoseni[2]

[1]Department of Chemistry and Industrial Chemistry, Bowen University, Iwo, Nigeria.
[2]Department of Biological Sciences, Bowen University, Iwo, Nigeria.

Received 8 February, 2018; Accepted 14 May, 2018

The indigenous African organic soap is formed by saponification. Using the local and ancient method, with slight modifications, palm kernel oil (*Elaeis guineensis)* and the filtrate of burnt cocoa pod ash (*Theobroma cacao)* were used to prepare African black soap ($C_{11}H_{23}COO^-K^+$). The prepared black soap was thereafter divided into five parts. Part A was the control without additives, while parts B, C and D were enhanced with aloe vera, camwood and lime respectively. Part E was enhanced with both shea butter and camwood. These samples were analyzed chemically by pH determinations, infrared spectroscopic analyses and phytochemical screenings. They were also screened for *in-vitro* antibacterial activities against two Gram-positive bacteria (*Staphylococcus aureus* and *Bacillus subtilis*) and two Gram-negative bacteria (*Pseudomonas aeruginosa* and *Escherichia coli*). The pH determinations showed that all the samples were alkaline in nature with values between 8.7 and 9.1. Infrared spectra analyses of the unenhanced black soap revealed a medium and a strong band due to υ (C=O) frequency of the keto group at 1740 and 1562 cm^{-1} respectively and a medium band at 1119 cm^{-1} due to υ (C-O) frequency of the ester oxygen. These bands appeared almost unchanged in the Infrared spectra of the enhanced samples signifying no complexation through the oxygen donor atoms. Thus, the structure of the black soap (A) was intact and it was not denatured by the various additives. Phytochemical screenings revealed that A and D contained saponins, flavonoids and terpenoids; C contained both flavonoids and terpenoids; B and E contained only terpenoids; while tannins and steroids were absent in all the samples. Antimicrobial studies showed that the enhanced black soap were either active against one or both gram-negative bacteria. In addition B, C and D were also active against either one or both gram-positive bacteria. E was inactive against the gram-positive bacteria, while the unenhanced black soap remained inactive against all tested organisms.

Key words: Enhanced African black soap, chemical, phytochemical and antimicrobial activities.

INTRODUCTION

African black soap or black soap, also known as *Alata Samina* or *Alata* originated from West Africa (Bella, 2008). It has being used since ancient time in Ghana and Nigeria, where it also enjoys several names like *Ose Dudu*, *Eko Zhiko* and *Sabulon Salo* (Getradeghana, 2000). This indigenous African organic soap is formed by

esterification (Bella, 2008). It has found a wide application for all household cleaning purposes from bathing to washing and cleaning (Getradeghana, 2000). Black soap enjoys a good reputation for its ability to deeply cleanse the skin's pores, remove blemishes and makeup, improve or eliminate uneven skin tone, razor bumps caused by ingrown hairs and skin rashes (Getradeghana, 2000). It is not scented and therefore can be used by anyone who wishes to improve the quality of his/her skin (Getradeghana, 2000). We have previously reported the preparation of African black soap by reacting palm kernel oil and the filtrate of burnt cocoa pods (the ash). The chemical analyses of the black soap revealed moisture content was 26% (w/w); Total Fatty Matter (TFM) was 44.75% (w/w), Total Fatty Alkaline (TFA) was 0.22% (w/w), Total Alkaline (TA) was 11.78% (w/w) and pH was 10 (Ikotun et al., 2017a). Some metal complexes were thereafter prepared by the reaction of the prepared black soap with some transition metal salts. The characterization of the black soap and prepared complexes done by spectroscopic analyses and determination of physicochemical properties revealed that the potassium salt ($C_{11}H_{23}COO^{-}K^{+}$), commonly called African black soap, acted either as a monodentate or bidentate ligand forming metal complexes by coordinating through one or two of its oxygen donor atoms and also by entirely replacing the potassium ion with the transition metal (displacement reaction). Our interest in this indigenous African black soap has previously led to studies using the ash from the sun dried cocoa pods (Ikotun et al., 2017b). This present work was aimed at preparing African black soap using the waste material from cocoa (cocoa pod burnt to ash without prior sun drying) and palm kernel oil. Thereafter, the different portions of the prepared black soap were enhanced with some naturally occurring beautifying organic compounds and analyzed chemically. Also, phytochemical analysis and *in-vitro* antimicrobial studies were carried out on them. This literature therefore serves as the first report on the physicochemical analyses, phytochemical analyses and antimicrobial studies of burnt cocoa pod filtrate prepared African black soap, as well as that of its enhanced samples with some skin-nourishing natural products.

MATERIALS AND METHODS

Chemical

Palm kernel seeds and cocoa pods were locally sourced from a town called Ifeodan, Osun State, Nigeria. All solvents used were purchased as analytical grades from Sigma-Aldrich and SAARChem

Instrumentation

The Infrared spectra were recorded as KBR plates on a Nicolet Avatar FTIR 330 spectrophotometer. Hanna Professional Waterproof pH/ORP meter was used for determining the pH.

Preparation of the black soap

African Black soap was prepared according to literature (Ikotun et al., 2017b) and divided into five portions. Some beauty enhancing natural compounds were added as additives into four of the soap portions in separate labeled containers, followed by manual pounding with a pestle and mortar. Part A was without additives, while part B contained 12.50 g of black soap pounded with half table spoon of squeezed aloe vera. Sample C contained 12.50 g of black soap pounded with 0.7 g cam wood. Sample D contained 12.50 g black soap pounded with 7 drops of lime. Part E was enhanced by pounding 12.50 g black soap with 0.35 g shea butter and 0.35 g camwood. These samples were analyzed by pH determinations, infrared spectroscopic analyses and phytochemical screenings.

Antimicrobial test

15.2 g of Mueller Hinton agar was measured into a 500-ml conical flask, 400 ml of distilled water was added and mixed/shaken till it dissolved, it was then covered with cotton wool and aluminum foil paper and labeled. It was autoclaved at a temperature of 121°C for 15 min. The agar was allowed to cool to a temperature of 45°C and aseptically poured into sterile Petri dishes. The poured agar was allowed to solidify. 0.5 g of the prepared samples and 2.5 ml of distilled water were dispensed into Mac Cartney bottles and allowed to dissolve. Sterile filter paper disc (7 mm in diameter) was then placed inside the dissolved soap mixture and allowed to soak for 10 min. The plates were then inoculated with the test bacteria using the spread plate method with a sterile swab stick. The test bacteria were two Gram-positive bacteria (*Staphylococcus aureus* and *Bacillus subtilis*) and two Gram-negative bacteria (*Pseudomonas aeruginosa* and *Escherichia coli*) (Cheesbrough, 2002; Emeruwa, 1982). The inoculated plates were kept on the work bench for 1 h before further work was carried out. The soaked discs were picked using forceps sterilized by flaming and placed aseptically on the inoculated Petri dishes. The discs were allowed to stick on to the surface of the agar medium before incubation. The plates were incubated at 37°C for 24 h and antibacterial activity of the soap was measured as diameter of zones of inhibition surrounding the impregnated filter paper discs. Zones of inhibition were measured in mm (Bauer et al., 1996; Balogun and Owoseni, 2013).

RESULTS AND DISCUSSION

Dunn (2011) reported the equation for the preparation of black soap as Equation 1, while Figure 1 presents its structure (Ikotun et al., 2017b).

*Corresponding author. E-mail: ikotunadebomi@gmail.com , lhbcards@yahoo.com.

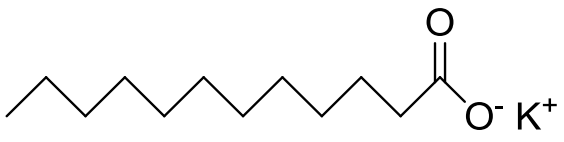

Figure 1. Structure of African Black Soap ($C_{11}H_{23}COO^-K^+$).

Table 1. pH values of the soap samples.

Samples	pH
A	8.9
B	8.7
C	9.1
D	8.9
E	8.9

Sample A , black soap alone; sample B, black soap with aloe vera; sample C, black soap with camwood; sample D, black soap with lime; sample E, black soap with sheabutter and camwood.

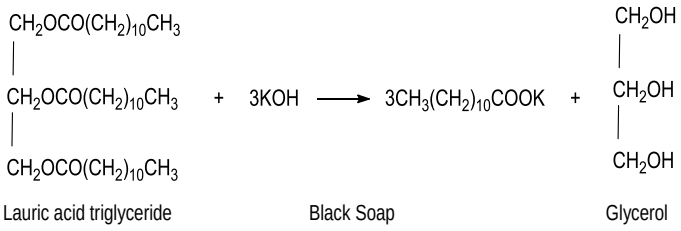

Equation 1: Preparation of African black soap.

pH determinations

Table 1 presents the pH values of the black soap and its enhanced samples. The pH determinations showed that all the samples were alkaline in nature with values between 8.7 and 9.1. Tarun et al. (2014) stated that majority of soaps have a pH value between 9 and 10.

FTIR spectra analyses

The FTIR spectra of the African black soap (Figure 2) and its enhanced samples (Figures 3 to 6) have been analyzed and presented as Table 2. The characteristic vibrational frequencies have been identified by comparing the spectra of the prepared African black soap with the enhanced samples (Ikotun et al., 2017a). The broad medium band at 3381 cm^{-1} in sample A was assigned to the stretching vibration of OH. This band shifted to a lower frequency of 3374 cm^{-1} in samples B and E, while appearing at 3376 cm^{-1} in C and at 3364 cm^{-1} in D. The spectrum of A showed the sp^3 C-H stretching vibrations at 2920, 2957 and 2863 cm^{-1}, respectively. These bands have also appeared at about the same frequencies in all its enhanced samples. The stretching vibrational frequency of C=O for sample A appeared as a medium and a strong band at 1740 and 1562 cm^{-1}. These bands have appeared unchanged in all other samples. The stretching vibrational frequency of C-O of sample A was assigned the value 1119 cm^{-1}. The band appeared unchanged in samples B and C, but shifts to a slightly lower frequency at 1117 cm^{-1} in samples D and E. This analysis shows that the structure of black soap is intact and it was not denatured by the various additives.

Phytochemical screenings

The results of the phytochemical screenings of all the black soap samples are presented below as Table 3. The results showed that samples A and D contained saponin, while all the samples contained terpenoids. Sample C contained flavonoids, while tannins and steroids are absent in all the samples. These results revealed the presence of some essential secondary metabolites which nourish the skin.

Antimicrobial screenings

The results of the antibacterial activities of the black soap and its enhanced samples are displayed in Figure 7. Sample B, which contained aloe vera, was active against both Gram-positive bacteria, as well as *E. coli*. Sample C, which contained camwood, was active against *S. aureus* and *E. coli*. Sample D, which contained lime, was active against both Gram-negative bacteria and the only one active against *P. aeruginosa.* It was also active against *S. aureus.* Sample E, which contained shea butter and camwood, was only active against the *B. subtillis*. African black soap remained inactive against all tested microorganisms.

Conclusion

The results of the phytochemical screenings of black soap revealed it contains some secondary metabolites which are nourishing to the skin. This is a good justification for the reason it cleanses deeply and nourishes all skin types. The enhancement of black soap with some other natural skin beautifying compounds did not affect or denature it, but rather facilitated its antimicrobial activities.

CONFLICT OF INTERESTS

The authors have not declared any conflict of interests.

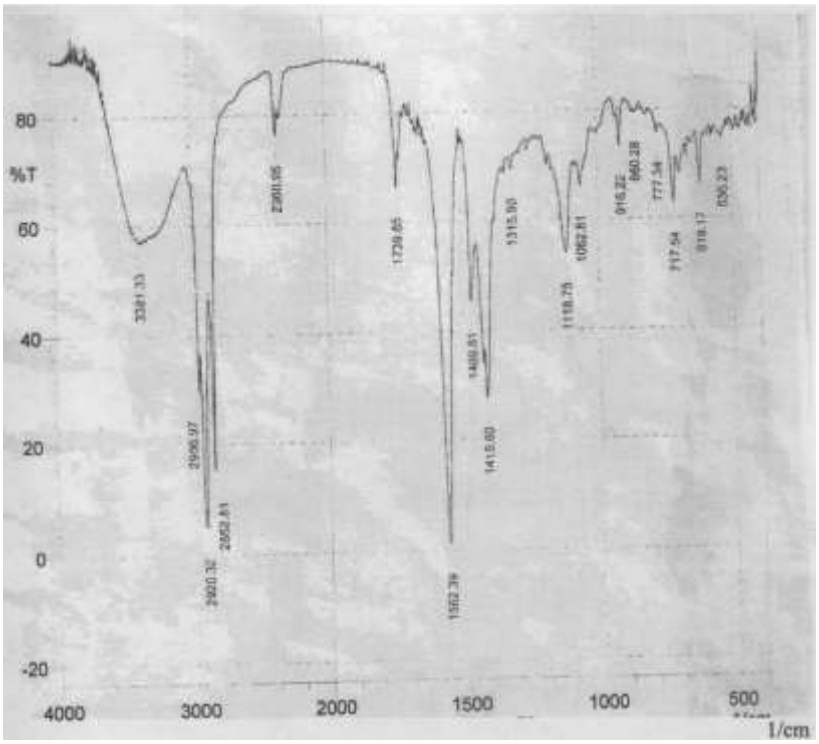

Figure 2. FTIR spectrum of the black soap without enhancement (Sample A).

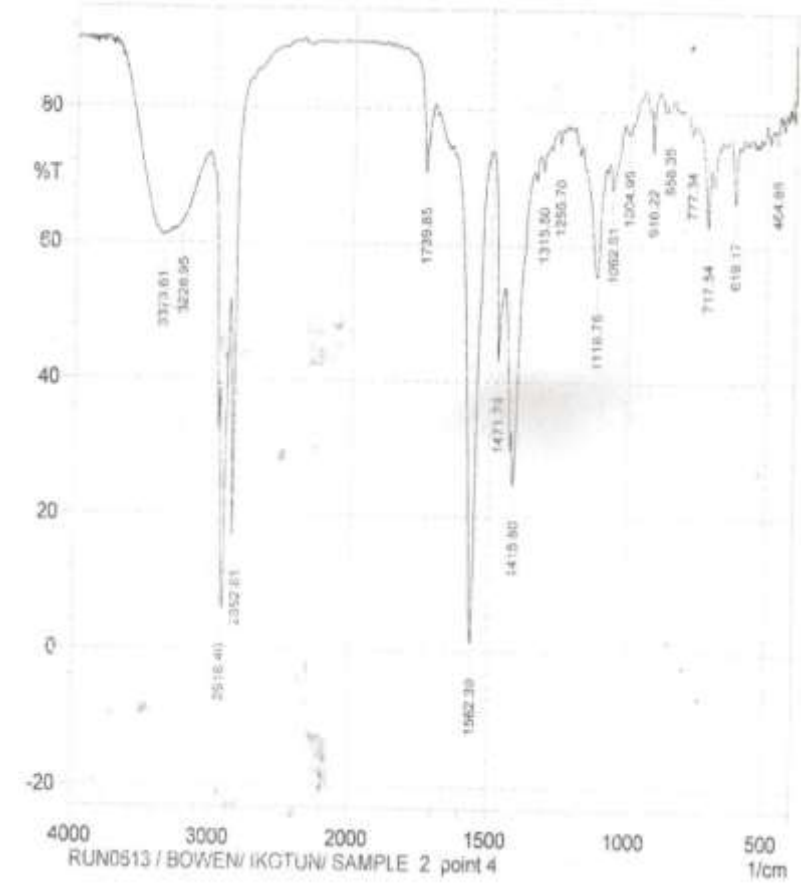

Figure 3. FTIR spectrum of B (Black soap with aloe vera).

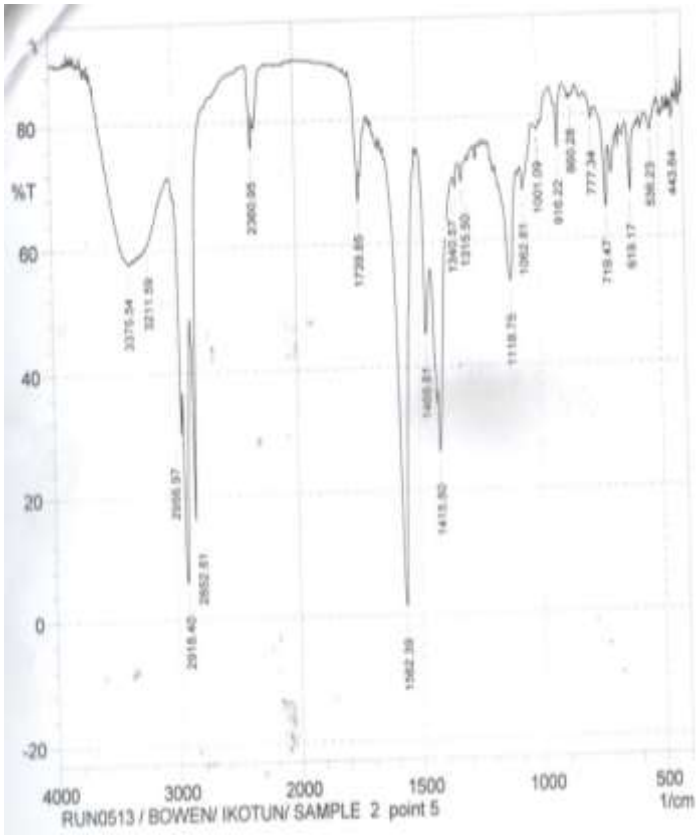

Figure 4. FTIR spectrum of C (black soap pounded with camwood).

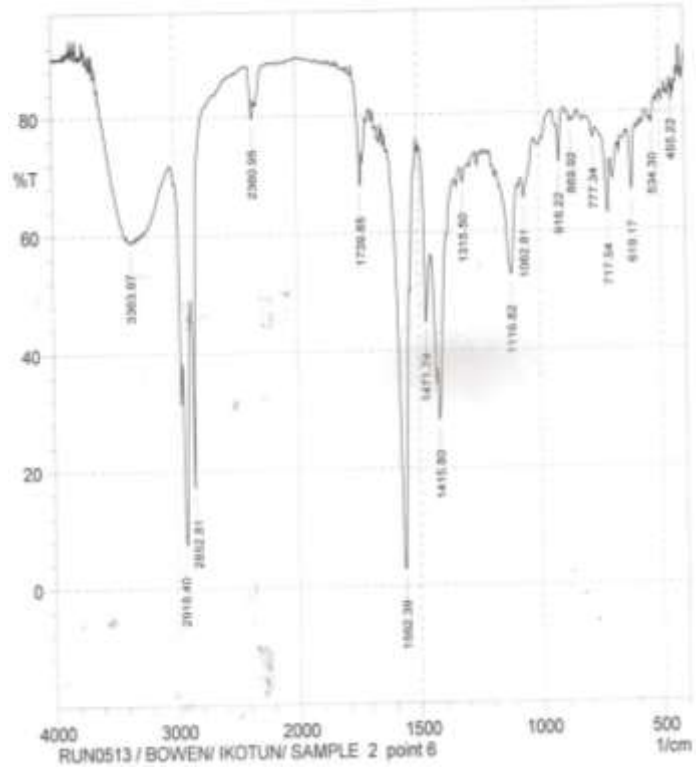

Figure 5. FTIR spectrum of D (black soap with lime).

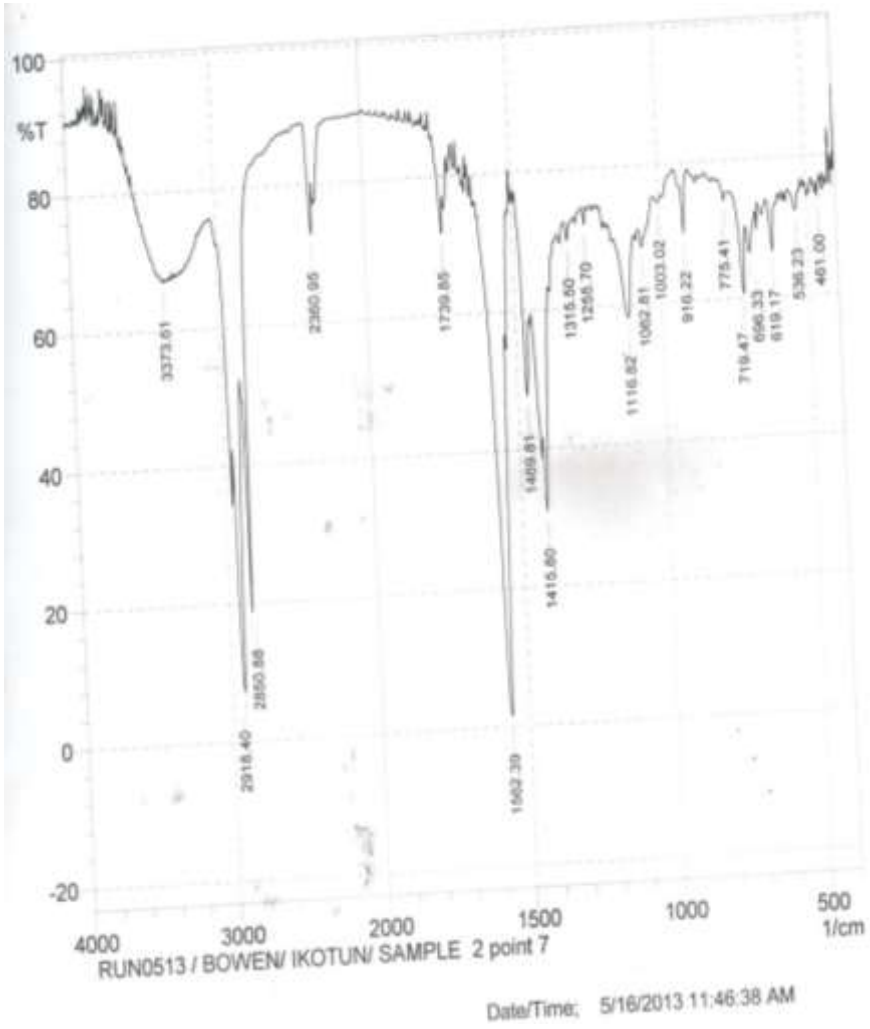

Figure 6. FTIR spectrum of E (black soap with shea butter and camwood).

Table 2. FTIR spectra analyses of black soap and its enhanced samples.

Sample	υ (OH) (cm^{-1})	υ (C-H) (cm^{-1})	υ (C=O) (cm^{-1})	υ (C-O) (cm^{-1})	Others
A	3381 bm	2920 s 2957 sh 2863 s	1740 m 1562 s	1119 m	1416s
B	3374 bm	2918 s 2853 s	1740 m 1562 s	1119 m	1416 s
C	3376 bm	2918 s 2957sh 2853 s	1740 s 1562 s	1119 m	1416 s
D	3364 bm	2918 s 2853 s	1740 m 1562 s	1117 m	1416 s
E	3374 bm	2918 s 2851 s	1740 m 1562 s	1117 m	1416 s

s, Strong; m, medium; b, broad; bs, broad strong; bm, broad medium; sh, shoulder.

Table 3. Results for the phytochemical screenings of the black soap samples.

Sample	Tannins	Saponin	Flavonoids	Steroids	Terpenoids
A	-	+	+	-	+
B	-	-	-	-	+
C	-	-	+	-	+
D	-	+	+	-	+
E	-	-	-	-	+

+, Present; - , Absent.

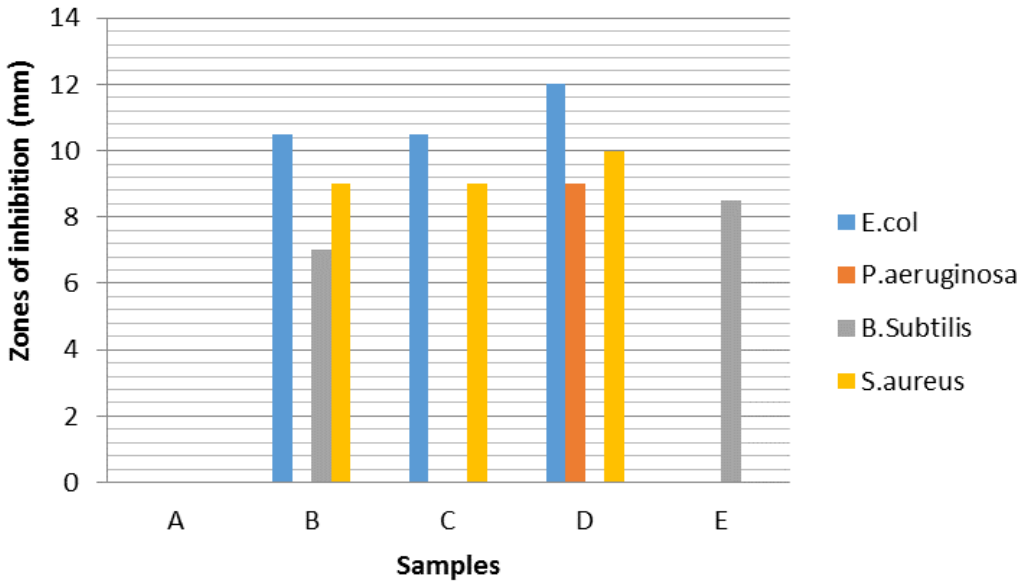

Figure 7. Antibacterial activities of black soap and its enhanced samples. *E. col = Escherichia coli; P. aeruginosa = Pseudomonas aeruginosa; B. subtilis = Bacillus subtilis ; S. aureus = Staphylococcus aureus.*

REFERENCES

Balogun OS, Owoseni AA (2013) Phytochemical and antimicrobial investigation of *Dissotis rotundifolia* (sm) Triana. Natural Products 9(2):77-80.

Bauer AW, Kirby WM, Sherris JC, Turck M (1996). Antibiotic susceptibility testing by a standardized single disk method. American Journal of Clinical Pathology 45:439-496.

Bella O (2008). African Black Soap, http://www.bellaonline.com/articles/art26846.asp.

Cheesbrough M (2002). Biochemical tests to identify bacteria. In. Laboratory practice in tropical countries. Cheesbrough M (ed.). Cambridge Edition pp. 63-87.

Dunn KM (2010). Scientific Soap making: The Chemistry of Cold Process. Clavicula Press.

Emeruwa KC (1982). Antimicrobial substances from Cacaya papaya fruit extracts. Journal of Natural Products 45:123-127.

Getradeghana BT (2000). Evaluation of African traditional soap. Global Journal of Pure and Applied Sciences 6:174-179.

Ikotun AA, Awosika OO, Oladipupo MA (2017a). The African Black soap from *Elaeis guinensis* (Palm Kernel Oil) and *Theobroma cacao* (Cocoa) and its transition metal complexes. African Journal of Biotechnology 16(18):1042-1047.

Ikotun AA, Olalere CA, Adekunle DO, Dawodu MO (2017b). Phytochemistry and Antimicrobial Studies of African Black Soap and its Modified Samples. Journal of Chemical and Pharmaceutical Research 9(5):354-359.

Tarun J, Susan J, Suria J, Susan VJ, Criton S (2014). Evaluation of pH of Bathing Soaps and Shampoos for Skin and Hair Care. Indian Journal of Dermatology 59(5):442-444.

Related Journals: